

# UCLA

## UCLA Previously Published Works

### Title

Structural Contributions to Autocatalysis and Asymmetric Amplification in the Soai Reaction

### Permalink

<https://escholarship.org/uc/item/75p8m9d3>

### Journal

Journal of the American Chemical Society, 142(43)

### ISSN

0002-7863

### Authors

Athavale, Soumitra V  
Simon, Adam  
Houk, KN  
[et al.](#)

### Publication Date

2020-10-28

### DOI

10.1021/jacs.0c05994

Peer reviewed



Published in final edited form as:

*J Am Chem Soc.* 2020 October 28; 142(43): 18387–18406. doi:10.1021/jacs.0c05994.

## Structural Contributions to Autocatalysis and Asymmetric Amplification in the Soai Reaction

Soumitra V. Athavale<sup>a</sup>, Adam Simon<sup>b</sup>, Kendall N. Houk<sup>b</sup>, Scott E. Denmark<sup>a,\*</sup>

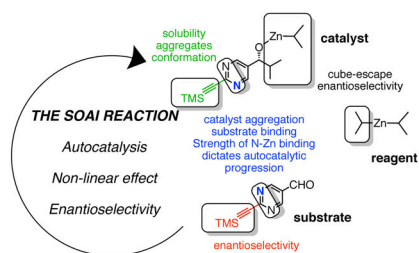
<sup>a</sup>Roger Adams Laboratory, Department of Chemistry, University of Illinois, Urbana, IL, 61801

<sup>b</sup>Department of Chemistry and Biochemistry, University of California, Los Angeles, CA 90095

### Abstract

Diisopropylzinc alkylation of pyrimidine aldehydes – the Soai reaction, with its astonishing attribute of amplifying asymmetric autocatalysis, occupies a unique position in organic chemistry and stands as an eminent challenge for mechanistic elucidation. A new paradigm of ‘mixed catalyst substrate’ experiments with pyrimidine and pyridine systems allows a disconnection of catalysis from autocatalysis, providing insights into the role played by reactant and alkoxide structure. The alkynyl substituent favorably tunes catalyst solubility, aggregation and conformation while modulating substrate reactivity and selectivity. The alkyl groups and the heteroaromatic core play further complementary roles in catalyst aggregation and substrate binding. In the study of these structure activity relationships, novel pyridine substrates demonstrating amplifying autocatalysis were identified. Comparison of three autocatalytic systems representing a continuum of nitrogen Lewis basicity strength suggests how the strength of N-Zn binding events is a predominant contributor towards the rate of autocatalytic progression.

### Graphical Abstract



\*Address Correspondence to: Professor Scott E. Denmark, 245 Roger Adams Laboratory, Box 18, Department of Chemistry, University of Illinois, 600 S. Mathews Ave, Urbana, IL 61801, tel: (217) 333-0066, sdenmark@illinois.edu.

#### Supporting Information

The Supporting Information is available free of charge on the ACS Publications Website.

Full experimental details and characterization data along with descriptions of ancillary experiments.

The authors declare no competing financial interest.

## INTRODUCTION

### 1. Asymmetric Autocatalysis and the Soai Reaction.

The diisopropylzinc alkylation of pyrimidine-carboxaldehydes, crowned the Soai reaction (Figure 1) represents an astonishing and fortuitous confluence of three themes in catalysis: (1) autocatalysis, (2) enantioselective catalysis and (3) positive non-linear effects. Each product enantiomer catalyzes its own formation (selective autocatalysis) while also inhibiting catalysis by its counterpart (a positive non-linear effect) – resulting in a continuous amplification of the excess enantiomer with reaction progression. Soai's seminal 1995 report described how the inclusion of scalemic product carbinol **1a** at the beginning of the reaction resulted in the newly-formed product being more enantioenriched than the initial additive.<sup>1,2</sup> Near racemic autocatalyst with only 51:49 e.r. provided a higher enantioenriched product with 55:45 e.r. The product from one reaction was used as the catalyst for a subsequent reaction and it was shown that in successive reaction cycles, the enantioenrichment of **1a** could be increased to up to 94.5:5.5 e.r. Following this discovery, it was demonstrated that in general, the reaction of diisopropylzinc with 2-substituted pyrimidinyl aldehydes displayed autocatalytic, asymmetric amplification.<sup>3–8</sup> In particular, a bulky alkynyl substituent (Figure 1b) drastically increases the performance of these reactions in terms of enantioenrichment achieved, reaction times and isolated yields. For example, the asymmetric autocatalytic reaction with **1d** affords the product in an enantiopure form in quantitative yield. Following this report, **1d** became the workhorse substrate for future studies by the Soai group. Curiously, replacement of the *t*-Bu group in **1d** by a triisopropylsilyl (TIPS) group (**1c**) was detrimental to asymmetric amplification.<sup>4</sup>

Although the theoretical framework for amplifying autocatalysis was articulated as far back as 1953 (the term 'asymmetric autocatalysis' itself was coined by Weinberg in 1989), the Soai reaction remains the only example of an autocatalytic, non-equilibrium, irreversible chemical transformation capable of robust asymmetric amplification.<sup>9,10</sup> With substrate **1d**, the reaction provides enantiopure products within three reaction cycles even when the autocatalyst used has a calculated e.e. as low as  $5 \times 10^{-5}$ %.<sup>11</sup> Investigations by Soai<sup>12–14</sup> and Singleton<sup>15,16</sup> have demonstrated that the Soai reaction is capable of producing a non-racemic product even in the absence of any added catalyst. This symmetry breaking arises from a statistical imbalance in the formation of the enantiomeric products in the early evolution of the reaction, which is subsequently propagated and amplified by asymmetric autocatalysis.<sup>9</sup> The Soai reaction is thus a successful example of absolute asymmetric synthesis.<sup>17</sup> A large variety of chiral additives ranging from amino acids,<sup>18</sup> enantiomorphous crystals,<sup>19</sup> helical hydrocarbons<sup>20</sup> and even cryptochiral molecules<sup>21</sup> can influence the outcome of the reaction by biasing an initial imbalance of one of the enantiomers.<sup>22</sup> Remarkably, even circularly polarized light<sup>23</sup> and isotopic chirality<sup>24–26</sup> have been demonstrated to result in a nonracemic product. One may state that in multiple cycles of the Soai reaction, symmetry breaking and enantioenrichment is inevitable. The Soai reaction hence qualifies as a chemical transformation with a predisposition to evolve toward homochirality. Soai's seminal discoveries have received widespread attention in diverse chemical fields and have revived discussions regarding absolute asymmetric synthesis, symmetry breaking and the origin of biological homochirality.<sup>27–31</sup> The interested reader is

directed to a number of reviews for further details, accounts and descriptions of the remarkable Soai system.<sup>17,22,32–35</sup>

## 2. The Soai Reaction as a Mechanistic Challenge.

More than two decades since Soai's initial discovery, fundamental questions regarding its mechanism have remained unanswered. The most obvious outstanding issues are the precise identity of the alkoxide autocatalyst, its genesis and propagation, the origin of its nonlinear behavior and a compelling transition state model accounting for generation of the homochiral product from the reactants.

Empirically, it is clear that the structural constraints on reactants are severe, but the basis for this narrow substrate scope remains enigmatic. In the dialkylzinc alkylations of pyridine-3-carbaldehyde (**3a**), inclusion of the scalemic product carbinol provides newly formed product that is not racemic but with a lower enantioenrichment than the additive.<sup>36</sup> The reports with pyrimidine-5-carbaldehydes without exception describe the use of only diisopropylzinc as the nucleophile. The incompetence of other dialkylzinc reagents is presumed, although systematic studies are lacking.<sup>37,38</sup> Soai et al. have described isolated reports wherein amplifying autocatalysis with diisopropylzinc was demonstrated with other substituted quinoline-3-carbaldehydes and 5-carbamoylpyridine-3-carbaldehyde.<sup>39–42</sup> However, pyrimidine-5-carbaldehydes remain the workhorse substrates for the reaction and among these, 2-alkynyl substituted aldehydes display superior autocatalysis and selectivities. TIPS-alkynyl substrate **1c** presents a remarkable exception to this trend and highlights the puzzling idiosyncrasies typical of the substrate scope of this transformation. The rationalization of these structural constraints poses a test to any mechanistic proposal.

The reaction is extremely sensitive to initial chiral imbalances, including the extraordinary susceptibility to additives with isotopic chirality and other cryptochiral additives. The fundamental chemical interactions between such additives and the reactants that ultimately trigger symmetry breaking remain poorly understood. Similarly, rationalization of the structural and kinetic boundary conditions assuring symmetry breaking in uncatalyzed reactions remains a key issue.<sup>43,44</sup>

The study of the Soai reaction also presents technical challenges including: (1) the dialkylzinc reagent is highly pyrophoric and moisture sensitive, complicating experiment design and execution, (2) the autocatalytic nature of the reaction demands nontrivial strategies for kinetic analysis, and (3) structural investigations maybe impeded by the stability and solubility of the zinc alkoxide intermediates. Thus, overall, the Soai reaction with its *sui generis* characteristics, presents unique challenges to mechanistic investigation. A holistic understanding of the reaction raises hopes of developing new transformations that may display amplifying asymmetric autocatalysis and potentially contribute to the understanding of the origin of homochirality in nature.

## 3. Current Mechanistic Consensus.

The striking properties of the Soai system have motivated numerous studies to elucidate the mechanism of this iconic transformation.<sup>34,38,45–52,37,53–61,43</sup> Because catalyst aggregation

is a central contributor to non-linear effects, investigations have predominantly focused on probing the aggregation states for the product zinc alkoxide. Early kinetic studies with the 3-formyl-6-methylpyrimidine-carbaldehyde system included a comparison between enantiopure and racemic autocatalyst and indicated a dimeric alkoxide aggregate as the catalytic species whereas further investigations, while subsequent investigations with an enantiopure catalyst suggested two aldehyde substrates in a tetrameric complex.<sup>45,48,58</sup> The first structural studies in 2004, deduced from <sup>1</sup>H NMR spectroscopy with the **2b**-derived isopropylzinc alkoxide are consistent with a dimeric model.<sup>49,50</sup> Note that these experiments cannot conclusively distinguish between dimers and higher order aggregates. Likewise, modeling studies indicated that the extraordinarily high experimentally observed amplification efficiency (especially for the alkynyl substituted systems) was not possible with dimeric catalysis and necessitated the invocation of higher order aggregates in the catalytic cycle.<sup>55,47,35</sup> Theoretical suggestions for possible higher order aggregate structures, including the square-macrocycle-square (SMS) tetramer were made for the first time by Gridnev and Brown.<sup>62,37</sup> Subsequent investigations provided further momentum for a tetrameric catalyst model. Reaction progress kinetic analysis (RPKA) experiments<sup>57</sup> with substrate **1e** indicated the reaction rate to be 0<sup>th</sup> order in diisopropylzinc, 1<sup>st</sup> order in catalyst (product alkoxide) and 1.6 order in aldehyde. An intriguing inverse temperature dependence on the reaction rate was also observed. On the basis of kinetic and spectroscopic clues, the suggestion that the SMS tetrameric alkoxide might be the active catalyst was raised for the first time. A DFT study to model these tetramers was subsequently reported by Gridnev in 2012.<sup>59</sup>

Finally in 2015, the first crystal structure of the isopropylzinc alkoxide derived from **2d** was published by Soai *et al.*<sup>60,61,63</sup> Depending on the conditions for crystallization, a tetrameric or oligomeric aggregate is obtained. The homochiral and heterochiral tetramers possess a 12-member macrocycle with a connectivity resembling the SMS tetrameric structure proposed earlier (Figure 2). The assembly can be considered as a concatamer of two Zn-O square dimers, ligated through pyrimidine-Zn coordination. In the homochiral tetramer, the unbound pyrimidine units (referred to as the tetramer 'arms') are oriented on the same face of the macrocycle. The racemic, heterochiral tetramer possesses a similar overall connectivity but the arms are placed on opposite sides of the macrocycle. In both the homochiral (enantiopure) and heterochiral (racemic) tetramers, a pair of three-coordinate, unsaturated (alkoxy)zinc atoms are present as part of the pyrimidinyl arms. The orientation of these unsaturated zinc centers follows the pattern of the arms. Finally, for both the tetramers, the crystal structure also showed that except for the two macrocycle residing nitrogen atoms, all the remaining six pyrimidinyl nitrogen atoms are bound by diisopropylzinc molecules (these are not shown in the structure in Figure 2). Soai's crystal structure elucidation is a landmark achievement in providing a definitive structural understanding of the solid-state SMS tetramer and revealing the differences in the homochiral and heterochiral tetrameric assemblies.

Two decades of investigations into the Soai reaction culminated in the identification of alkoxide tetramers as the likely autocatalysts. However, this knowledge had not provided insights into the mode of action of the catalyst nor a compelling transition state model or an

explanation of the structural constraints on the reactants. Recently, we addressed this central issue regarding the *modus operandi* of the autocatalyst.<sup>64</sup> These investigations, summarized in Figure 3, revealed the structural logic behind the assembly and working of the SMS tetrameric (auto)catalyst on the basis of the following key findings: (1) discovery of amplifying autocatalysis in the diisopropylzinc alkylation of the related pyridine substrate **3b** proved that only one nitrogen in the aromatic core is necessary for the Soai phenomenon (Figure 3a); (2) whereas related structures like **PyEE**, **PyEI** and **PyIE** predominantly form catalytically inactive, Zn-O cubic tetramers, the steric bulk of the product zinc alkoxide **PyII**, in combination with pyridyl-nitrogen coordination enables a ‘*cube-escape*’ pathway to an alternative, catalytically active tetrameric cluster sharing identical connectivity with Soai’s crystal structure (the SMS tetramer) (Figure 3b); (3) this cluster engages the substrate aldehyde through a two-point coordination (via the carbonyl oxygen and the aromatic nitrogen) to the unsaturated (alkoxy)zinc centers on the catalyst floor (highlighted in yellow in the ground state structures in Figure 3c), termed as the ‘*floor-to-floor*’ model; (4) the resulting activated aldehyde is alkylated by an activated diisopropylzinc molecule, delivered preferentially from only one of the catalyst arms, leading to the homomorphic product alkoxide (**TS-4b**) in Figure 3c; the competing transition state structure which leads to the heteromorphic product and is disfavored by 4.2 kcal/mol is not shown), comporting with an enantioselective, autocatalytic process; (5) such a *floor-to-floor* binding is structurally impossible for the thermodynamically preferred *heterochiral* **PyII** SMS tetramer (Figure 3c,  $G_{\text{rel}} = 0$ ) and the alternative single point binding pathway results in an energetic penalty for catalysis, hence providing a basis for the signature non-linear effect in the reaction. Overall, the *cube escape* – *floor to floor* catalysis model rationalizes both the genesis of the SMS tetramer, as well as its specific, non-linear, autocatalytic activity.

The current work complements and builds on these findings. Experiments providing specific insights into the structural contributions that affect asymmetric autocatalysis in the Soai reaction are described. Further subtle effects of the nitrogen Lewis basicity in controlling autocatalytic progression are uncovered by a comparison of the pyrimidine and pyridine systems.

#### 4. Research Plan and Rationale.

The asymmetric autocatalytic reaction of **1b** involves three components: the zinc alkoxide ‘catalyst’, the dialkylzinc ‘reagent’ and the aldehyde ‘substrate’. Each component may be divided intuitively into identifiable constituents (Figure 4). For example, at least four constituents of the catalyst are: (1) the alkylzinc counterion, (2) the carbinol group (isopropyl in this case), (3) the heteroaromatic core and, (4) the 2-alkynyl substituent. The aldehyde possesses fewer constituents, only the pyrimidine ring and the 2-substituent. No such deconstruction of the dialkylzinc component is possible. An overarching objective as the mechanistic investigations were inaugurated was, to holistically delineate the role played by these three components, and their structural constituents, in affecting catalysis, stereoselectivity, and nonlinearity in the reaction. Rate enhancement, enantioselectivity and a nonlinear effect are the most relevant properties of the alkoxide catalyst in combination with the dialkylzinc reagent. However, which structural constituents of the alkoxide affect these

properties was, at the outset, unclear. Likewise, the contributions from the aldehyde structural constituents that make it an ideal substrate for the catalyst were unknown.

Extracting meaningful structure activity relationships from a set of analogous autocatalytic reactions is challenging because a single structural change cannot be performed – both the (auto)catalyst and the substrate structures have to be modified at the same time. However, autocatalysis can be considered as a special case of catalysis wherein the substrate structure is ‘matched’ to generate a product that is catalytically active. From such a perspective, it is seen that catalysis, enantioselectivity and non-linearity arise as a result of the catalyst structure and can manifest in other reactions where the catalyst is operational, whereas autocatalysis is an incidental property emerging from a *matched* substrate structure. We hypothesized that individual contributions from the catalyst and the substrate can be studied independently from each other in a set of reactions where the (auto)catalyst and substrate structures are not *matched* but the substrates are nonetheless competent (in other words, the reaction is *catalytic but not autocatalytic*). Thus, combination experiments of various zinc alkoxides and aldehyde substrates were planned and are described in the upcoming sections. Figure 5 depicts the compound numbering scheme in these experiments.

## RESULTS AND DISCUSSION

### 1. Structure Activity Relationships in the Soai Reaction.

**1.1. In-situ IR Monitoring.**—To establish a reliable analytical method, the reactant combination of diisopropylzinc and pyrimidine-5-carbaldehyde **1b** was chosen as a model system for investigations. *In-situ* IR spectroscopic analysis was considered a convenient technique to monitor the transformation. A distinct advantage of this method over previously used *in-situ* monitoring strategies (calorimetry or NMR spectroscopy) is that the experimental setup allows for simultaneous manual sampling of the reaction mixture to determine product e.r. at any chosen time point. The aldehyde is added as the final component to the reaction mixture (this time is assigned as  $t = 0$ ) and the resulting carbonyl IR absorbance peak is tracked over time. Figure 5 depicts a typical data set obtained for such experiments. Combining **1b** with diisopropylzinc in the absence of catalyst led to a sigmoidal aldehyde decay with an initial induction period followed by rapid aldehyde consumption (entry 1). Inclusion of scalemic product carbinol as a catalyst in the reaction eliminates the induction period and results in a rapid reaction with higher final product e.r. (entry 2) Such behavior is typical for a reaction showing amplifying autocatalysis. In contrast, the same reaction with diethylzinc shows slow consumption in absence of added autocatalyst (entry 3). Inclusion of scalemic product results in enantiomeric erosion with no rate enhancement over the uncatalyzed reaction (entry 4). Thus, the reaction of **1b** with diethylzinc demonstrates no autocatalysis or chiral amplification. The surprising failure of the triisopropylsilyl analog, **1c** to display amplifying autocatalysis in reaction with diisopropylzinc was also examined. Indeed, in a series of *in-situ* IR monitored experiments with inclusion of the scalemic product carbinol as a catalyst, neither asymmetric amplification nor appreciable rate enhancement was observed over the sluggish background alkylation reaction, thus confirming Soai’s previous findings.<sup>65</sup> *In-situ* monitoring in

combination with manual sampling emerged as a convenient tool to interrogate catalysis and selectivity in the Soai reaction.

## 1.2 'Mixed Catalyst-Substrate' Experiments and the Discovery of Amplifying Autocatalysis with 5-(Trimethylsilylethynyl)pyridine-3-carbaldehyde.—

The investigation of the role of the aldehyde substrate constituents began with a study of the reaction of diisopropylzinc and various aldehydes with the isopropylzinc alkoxide of **2b**, henceforth denoted as **PmII** (nomenclature: *Pm/Py/Ph* = pyrimidine/pyridine/phenyl indicating the aromatic core, *I/E* = isopropyl/ethyl indicating the carbinol alkyl group and *I/E* = isopropyl/ethyl indicating the alkylzinc group, see Figure 5), as the catalyst (Figure 7). The aim of this survey was to determine if the catalyst-reagent combination of **PmII** and diisopropylzinc could successfully affect rate enhancement and positive non-linear enantioselectivity in the alkylation of aldehydes distinct from its 'natural' substrate **1b** and to simultaneously evaluate the effect of substrate structure on such an activity. The runs are 'mixed catalyst-substrate' experiments because the alkylation of the substrate produces a species distinct from the initial catalyst. Note that under these conditions, the uncatalyzed addition of diisopropylzinc to the test substrates is slow with low conversion. In Figure 7, the substrates are arranged in decreasing order of their rate of reaction and this convention continues in the subsequent figures.

For aldehydes **3b**, **3a**, **1c**, and **3c**, diisopropylzinc alkylation with scalemic **PmII** afforded products with e.r. significantly higher than the added catalyst (Figure 7). The relative rates of reaction were qualitatively in the order **3b** >> **3a** > **1c** > **3c**. *In contrast, no product was detected with the analogous phenyl substrates 5a and 5b.* The striking rate observed with **3b** motivated further detailed control experiments which revealed that in fact, the reaction of this substrate with diisopropylzinc displayed robust, amplifying, asymmetric autocatalysis! Thus, the high rate is attributable to an autocatalytic progression supported by the newly formed, catalytically competent product alkoxide. Such a possibility was rigorously ruled out for the other substrates. Thus, such mixed-catalyst experiments led to the discovery of the competent pyridine system, **3b**, and the subsequent *cube-escape, floor-to-floor* model summarized earlier.

Clearly, the signature characteristic of **PmII**, namely, catalyzed, positive-nonlinear, enantioselective addition of diisopropylzinc is also conserved in reactions with some 'unnatural' substrates (**3b**, **3a**, **1c**, and **3c**). However, it appears that for such a substrate to be competent, the minimal structural requirement is a 3-azaaryl group. In hindsight, these constraints are identical to ones described for the **PyII** tetramer autocatalyst,<sup>64</sup> a further confirmation of the striking similarity between the activities and mode of action of **PyII** and **PmII**. Note that the Gridnev transition state model<sup>59</sup> which discounts any interactions between the substrate nitrogen atoms and the unsaturated zinc atoms in **PmII** cannot be reconciled with the incompetence of **5a** and **5b**.

These results indicated that the alkyl transfer property of the Soai autocatalyst **PmII** could be studied in a manner which is disconnected from autocatalysis by providing a suitable surrogate substrate that does not produce an autocatalytically competent product. Comparison of **3c** with **3a** and **1c** respectively, suggests preliminary contributions of the



substrate structure independent of the (auto)catalyst attributes as: (1) increasing the bulk of the alkynyl substituent reduces the catalytic rate, (2) a pyrimidine substrate is more active than a pyridine and, (3) that these changes have a minimal effect on enantioselectivity of the catalytic transformation. Note that these conclusions specifically delineate substrate contributions to the overall catalysis by **PmII**.

In continuing the investigation of structural changes, the effect of the zinc alkoxide substituent was examined. The catalytic activity of alkoxide **PmIE** can be tested by including **2b** as an additive (resulting in the rapid formation of **PmIE** under reaction conditions) in the *diethylzinc alkylation* of various substrates. This species represents a combination in which the carbinol alkyl group (isopropyl) is distinct from the (alkoxy)zinc alkyl group (ethyl). The resultant mixed-catalyst experiments can hence show only conventional catalysis without a possibility of autocatalysis. The results of these catalyzed reactions proved to be extremely informative. Firstly, the control reactions of aldehydes **1b**, **3a**, **3b**, **1c** and **3c** showed no autocatalysis with diethylzinc (for example, in case of **1b**, see Figure 7). With inclusion of **PmIE**, varying efficiencies of catalytic diethylzinc alkylations were observed (Figure 8). With aldehyde **1b**, a significant rate enhancement and positive non-linear effect is seen (entry 1). The striking difference in the behavior of **1b** here, in comparison to results in entry 4, Figure 6 (which shows the lack of autocatalysis in the diethylzinc alkylation of **1b**, that is the catalytic incompetence of **PmEE**) demonstrates that a subtle change in the alkoxide structure from **PmEE** to **PmIE** turns on amplifying asymmetric catalysis *even with diethylzinc*. It thus appears that unlike **PmEE**, **PmIE** can potentially construct, at least to some meaningful degree, a catalytic structure similar to **PmII** (note that partial cube escape seen in case of **PyIE** must be also operative in case of **PmIE** – with the difference that the activity of the SMS tetramer in the latter is apparently high enough to affect catalysis). Rate and selectivity vary considerably with aldehyde structure (entries 2–5) and, a positive nonlinear effect is observed with all substrates except **3a** (entry 2). Only marginal catalysis was observed with the challenging TIPS-substituted substrates, **1c** and **3c** (entries 4, 5). As was the case in reactions with **PmII**, the phenyl substrates **5a** and **5b** were unreactive.<sup>65</sup> Although **3b** reacts more slowly than **3a**, the substituted pyrimidine **1b** is more reactive than either of these, suggesting that a balance of two opposing factors determine aldehyde reactivity: (1) the activating pyrimidine ring and, (2) the deactivating 2-alkynyl substitution. Likewise, comparison of entries 2, 3 and 5 suggests that the 2-alkynyl substituent improves substrate-controlled selectivity and among them, an optimum balance of reactivity and selectivity is achieved for aldehyde **3b**.

These conclusions strengthen and extend the trends deduced from Figure 7. In terms of rate and selectivity, comparison of analogous reactions in Figures 7 and 8 suggests that **PmII**-diisopropylzinc as a catalyst-reagent combination is superior to **PmIE**-diethylzinc. The reduction in activity of the latter allows identification of substrate effects, which are otherwise masked in case of highly efficient catalysis with the former.

Poor catalysis and asymmetric erosion was observed with **PmEE** catalyzed ‘mixed-catalyst substrate’ diethylzinc alkylations.<sup>65</sup> This behavior is consistent with the prediction that **PmEE** will predominantly exist as a catalytically inactive cubic tetramer. Finally, activity of

**PmEI** could not be unambiguously established because insolubility of this alkoxide precluded reliable estimation of catalyst concentration in solution.

**1.3. An Empirical Structure-Activity Correlation.**—A qualitative assignment of the contribution of structural constituents in the Soai reaction emerges from the results of the mixed catalyst-substrate experiments. Before elaborating on these assignments, it is instructive to restate the inferences gained through the **PyII** *floor-to-floor* transition-state model described in our previous work:

1. The bulky isopropyl groups enable cube escape from the catalytically inactive cubic tetramer.
2. Only a single nitrogen atom is necessary in the aromatic core to assemble the autocatalytically active SMS tetramer.
3. The SMS tetramer can process substrates belonging to the pyridine-3-carbaldehyde scaffold; the aromatic nitrogen is indispensable for two-point binding.
4. The substrate alkynyl substituent increases alkyl transfer enantioselectivity by disfavoring the minor transition state through an unfavorable steric interaction.

Results of the mixed catalyst-substrate experiments with **PmII** and **PmIE**, while being consistent with all the above conclusions provide additional inferences to this list:

5. The substrate alkynyl substituent decreases reactivity (while increasing selectivity).
6. The pyrimidine substrates are more reactive, presumably because of their increased electrophilicity in comparison to the pyridine substrates.
7. Diethylzinc, *in principle*, can be accepted as a reagent by the SMS tetramer to affect carbonyl alkylation, albeit with lower enantioselectivity, as compared to diisopropylzinc.

A case for the role of the *alkoxide alkynyl substituent* can be made from the following observations:<sup>65</sup> (1) the reaction of pyridine-3-carbaldehyde (**3a**) with diisopropylzinc does not show amplifying autocatalysis and the product alkoxide is poorly soluble, (2) in our hands, the reaction of pyrimidine-5-carbaldehyde (**1a**) with diisopropylzinc shows asymmetric amplification but with a lower potency than the alkynyl analogs, with the product alkoxide being poorly soluble, and, (3) the alkylation reactions of **3a** and **1a** are heterogenous; precipitation of the product alkoxide is observed early in the reaction. *In-situ* monitoring of the diisopropylzinc alkylation of **1a** did not give a sigmoidal profile despite being autocatalytic, perhaps because alkoxide precipitation results in a constant solution state catalyst concentration. The alkynyl substituent acts favorably by increasing the solubility of the product alkoxide as well as by minimizing formation of unproductive network aggregates by providing a steric shield on one side of the molecule. Thus, **3a** is autocatalytically incompetent owing to formation of insoluble, unproductive aggregates of the product alkoxide. Such an aggregation is presumably mitigated in case of **1a** because of weaker binding interactions of the pyrimidine nitrogen, allowing the maintenance in solution

of a critical concentration of active catalyst necessary to promote asymmetric amplification. It is important to note that precipitation is not the fundamental cause of autocatalytic amplification in the Soai reaction (reactions with the stalwart, highly efficient alkynyl substituted substrates, for example **1b** and **3b** are homogenous). However, precipitation effects may play an additional role in some cases — for example with **3a**, our observations (and comparisons with reaction of a **1a**) suggest that poor solubility of the product alkoxide contributes unfavorably.

To gain further insight into the incompetence of **3a** to undergo amplifying autocatalysis with diisopropylzinc, *floor-to-floor* transition states for alkyl transfer to **3a** by the expected SMS tetramer arising from the isopropylzinc alkoxide of **4a** (termed **NII**, equivalent to **PyII** minus the trimethylsilylalkynyl substituent – thus representing the theoretical autocatalytic alkylation of **3a** by diisopropylzinc) were computationally modeled (Figure 9). Transition structure **TS1** leading to the heterochiral (*R*)-**4a** product is slightly favored (0.2 kcal/mol) in comparison to **TS2**, which leads to the homochiral (*S*)-**4a** product. In contrast to the **PyII** system, these transition structures are almost isoenergetic, implying a poorly enantioselective alkyl transfer by the **NII** tetramer. Hence, the diisopropylzinc alkylation of **3a** does not show amplifying autocatalysis for at least two reasons: (1) the poor solubility of the product alkoxide and, (2) the poor enantioselectivity of the **NII** SMS tetramer (the solution concentration of which is already depleted due to poor solubility) catalyzed alkyl transfer pathway. On the basis of these results, the structure-activity inference list is extended further:

8. From the perspective of the autocatalyst, the alkynyl substituent contributes to efficient, enantioselective activity by: (a) improving solubility characteristics, (b) directing the alkoxide away from unproductive aggregates by providing a steric shield on one side of the molecule, and, (c) favoring a specific conformation of the SMS tetramer that increases enantioselectivity to meaningful levels.

The incompetence of substrates **1c** and **3c** (containing the triisopropylsilylalkynyl substituent, both these systems are highly soluble) in the Soai reaction is among the most bewildering idiosyncrasies of the Soai system. However, the mixed-catalyst substrate experiments demonstrated that both of these were competent substrates for the **PmII** (Figure 7), **PmIE** (Figure 8) and **PyII**.<sup>65</sup> Clearly, these aldehydes can undergo positive, non-linear enantioselective alkylation with a *viable SMS tetramer*. Thus, it can be concluded that the TIPS substituent maintains substrate competence but renders the corresponding SMS tetramer (derived from isopropylzinc alkoxides of **2c** and **4c**) inactive, hence impeding autocatalysis. Spectroscopic studies indicate that the isopropylzinc alkoxide of **4c** exists as a tetramer.<sup>65</sup> It is believed that this tetramer may exist in a highly hindered SMS conformation, which precludes substrate approach and binding.

Taken together, these conclusions paint a qualitative picture of the contributions of various structural components in the Soai reaction towards effecting amplifying asymmetric autocatalysis and are summarized in Figure 10.

## 2. Investigating Asymmetric Autocatalysis with Pyridine-3-carbaldehyde Derivatives.

The observation of amplifying, asymmetric autocatalysis with **3b** stimulated a survey of diisopropylzinc alkylations of other substituted pyridine-3-carbaldehyde (nicotinaldehyde) derivatives (Chart 1). Compounds with substituents at either the 5- or 6-position, as well as 5,6-disubstituted substrates were tested.

Aldehydes **7**, **8**, **9**, **10** and **14** were obtained from commercial sources whereas **11**, **12**, **13** and **15** were prepared by Suzuki-Miyaura or Sonogashira coupling reactions of the parent 6-bromonicotinaldehyde.<sup>6</sup> Aldehydes **16**, **17** and **18** were accessed by routes originating from 5-bromonicotinaldehyde (**14**) and involved the common intermediate 5-bromo-6-iodonicotinaldehyde (**21**) (Scheme 2). Deprotonation of the known dioxolane derivative **20** with tetramethylpiperidinylmagnesium chloride-lithium chloride<sup>66</sup> followed by trapping with iodine afforded the key intermediate **21**. Sonogashira coupling of **21** with 1.0 equiv ethynyltrimethylsilane afforded **22** in high yield which, after dioxolane deprotection provided target aldehyde **16**. Likewise, Sonogashira coupling of **21** with excess ethynyltrimethylsilane and subsequent dioxolane deprotection in a single pot allows direct access to **17**. The 5-methyl substituent was introduced by a Kumada coupling of **22** and methylmagnesium chloride and was followed by dioxolane deprotection to afford **18** in good yield. Buchwald (*t*-Bu<sub>3</sub>P)<sub>2</sub>Pd-G3 precatalyst was uniquely successful in the Kumada coupling whereas other palladium-ligand combinations gave poor yields.

A similar strategy to access **19** was unsuccessful because treatment of the protected dioxolane obtained from **23** (3-(1,3-dioxolan-2-yl)-5-fluoropyridine) with a variety of bases followed by trapping with iodine predominantly yielded iodination at the 4-position. Thus, the triisopropylsilyl ether **24** was utilized for iodination with tetramethylpiperidinylmagnesium chloride-lithium chloride and iodine. Carbinol **25** obtained in this way was alkynylated under Sonogashira coupling conditions to yield **26**. Finally, Swern oxidation of **26** afforded the target aldehyde **19** in high yield.

In a series of *in-situ* IR monitored reactions, each aldehyde was tested for asymmetric autocatalysis by inclusion of the corresponding scalemic product carbinol in the diisopropylzinc alkylation reaction. These reactions were compared to background reactions without any added product. In general, most of the substrates in Chart 1 displayed poor autocatalytic rate enhancement compared to the background reaction.<sup>65</sup> Apart from **3b**, amplifying asymmetric autocatalysis was observed only with **12**, **16**, **18** and **19**.

Reaction of substrate **12** without added catalyst (entry 1, Figure 11) shows sigmoidal aldehyde consumption. Inclusion of scalemic product carbinol (entry 2), results in drastic rate acceleration with the product carbinol being more enantioenriched (91:9 e.r.) than the added catalyst (71:29 e.r.). These results contradict a report by Amedjkouh et. al. wherein this transformation was reported to proceed with enantiomeric erosion.<sup>67</sup> From our perspective, Amedjkouh et. al.'s findings of enantiomeric amplification in the diisopropylzinc alkylation of **12**, with **2b** as the catalyst are consistent with **12** itself being autocatalytically competent.

Reactions of 5,6-disubstituted nicotinaldehyde substrates **16** and **18** with diisopropylzinc show asymmetric amplification under autocatalytic conditions, however the rate enhancement compared to the background reaction is only modest (Figure 12, entries 1–4). In case of **16**, a number of unidentified side products were observed. Qualitatively, the reaction of **18** appears to be more efficient with cleaner conversion and a higher final product e.r. Similar experiments with substrate **17** led to poor conversion and multiple side products without any asymmetric amplification in the target carbinol.<sup>65</sup> Conversely, autocatalyzed diisopropylzinc alkylation of **19** proceeded with robust asymmetric amplification and high rate enhancement compared to the background reaction (Figure 12, entries 5–6), mirroring the behavior seen with substrate **3b**. This outcome demonstrates that in the diisopropylzinc alkylations of 6-trimethylsilylethynyl-nicotinaldehydes, increasing the bulk of the 5-substituent adversely affects asymmetric autocatalytic behavior. The autocatalytic isopropylzinc alkoxide generated in the reaction with substrate **19** is labeled **FPyII** (*FPy* = fluoropyridine, *I* = isopropyl) is discussed below.

### 3. A Comparison of PmII, PyII and FPyII Systems.

**3.1. Comparison of Initial Rates with Nicotinaldehyde.**—The autocatalytic systems arising from substrates **1b**, **3b** and **19** differ only in the heteroaromatic core. The pyrimidine nitrogen, with lower Lewis basicity than the pyridine,<sup>68,69</sup> is expected to display weaker binding to the Lewis acidic diisopropylzinc reagent as well as to the O-Zn moiety. Likewise, the **FPyII** nitrogen should be less Lewis basic than the **PyII** nitrogen (pKa: pyridine = 5.23, 3-fluoropyridine = 3.0, pyrimidine = 1.30).<sup>68,70</sup> The comparison of these three systems thus provides an interesting opportunity to study the effects of such electronic changes on the autocatalytic behavior. To compare the inherent activities of the three alkoxide catalysts (**PmII**, **PyII** and **FPyII**) derived from these substrates, a comparison of initial rates with a common substrate, pyridine-3-carbaldehyde (**3a**) was undertaken.

Diisopropylzinc alkylation reactions under identical conditions were evaluated in the presence of 10 mol % of the alkoxide catalyst, with *in-situ* IR monitoring of aldehyde consumption. Initial rates were calculated and are reported as averages of three replicates (Figure 13). The three catalysts provide the product carbinol in comparable enantioenrichment. However, initial rates of **FpyII** and **PmII** while comparable to each other, are at least twofold lower than the rate with **PyII**. This observation may be rationalized by taking into account the *floor-to-floor* TS model for the alkyl transfer step. The transferring diisopropylzinc in the **PmII** and **FPyII** tetramer is deactivated (as compared to **PyII**) because of the weaker Lewis basicity of the coordinating nitrogen, resulting in a slower elementary alkyl transfer step. Thus, for an identical substrate, the activities of the three catalysts are in the order **PyII** > **PmII** ~ **FPyII**.

**3.2. Comparison of Autocatalytic Behavior.**—Autocatalytic reactions of substrates **1b** (**PmII** system), **3b** (**PyII** system) and **19** (**FPyII** system) were compared with inclusion of 8 mol % of initial autocatalyst. Under these conditions, rate of reaction in the **PyII** system is faster than the **FPyII** system (Figure 14) but significantly slower than the **PmII** system. While the **PmII** system reaction is nearly complete within one minute, less than 10 % conversion is seen for the other two at this time point. In these experiments, each

autocatalyst interrogates a different substrate and thus, the alkyl transfer rate is also affected by changes in the electrophilicity of the substrate aldehyde. On the basis of the increased electron-withdrawing effect of a pyrimidine ring and a fluoropyridine group in comparison to an unsubstituted pyridine core, **1b** and **19** are expected to be more electrophilic than **3b**. This conflicting balance of catalyst Lewis basicity and substrate electrophilicity must determine the overall rate of alkyl transfer in the three systems. With this perspective, the relative rates of the **PyII** and **FPyII** system appear reasonable. However, the extraordinarily high rate of the **PmII** system compelled further investigations into factors affecting autocatalytic progression.

**3.3. Inhibition of Autocatalysis by Excess Diisopropylzinc.**—The **PyII** system resembles many aspects of the autocatalytic **PmII** system.<sup>64</sup> However, studies probing the effect of excess dialkylzinc reagent led to the discovery of an unexpected divergence in the behavior of the two systems. Consistent with earlier reports,<sup>57</sup> autocatalytic progression of the **PmII** system was found to be insensitive to diisopropylzinc concentration but, similar experiments with the **PyII** system resulted in inhibition of reaction progression with increasing reagent concentration. This phenomenon was also noted for the **FPyII** system. Increasing diisopropylzinc concentration also adversely affected the selectivity of the reaction, presumably by accelerating the uncatalyzed background addition while concomitantly compromising the catalytic pathway.

Figure 15 presents the results of these comparative experiments (all runs are reproducible and represent one among duplicate experiments). The reactions of the three systems were carried out under identical conditions, with varying concentration of diisopropylzinc. The yellow curves represent reactions with the **PmII** system, which are extremely rapid, invariant in rate with respect to diisopropylzinc concentration, and provide the product with >99:1 e.r. in all cases. Reaction profiles with the **PyII** and **FPyII** system are represented by solid and dashed curves respectively. The autocatalytic reaction of **PyII** was inherently faster than that of **FPyII** at lower concentrations of zinc reagent (compare entries 1 and 5, also see Figure 14). However, with increasing diisopropylzinc concentration, reactions of the former were inhibited more significantly than the latter (entries 1 to 8). Thus, at diisopropylzinc concentrations upward of 2.4 equivalents, the **FPyII** reactions were faster than those of **PyII** (compare entries 2 and 6, 3 and 7, 4 and 8). These results demonstrate that the extent of inhibition by excess diisopropylzinc is greater for **PyII** than for **FPyII** and is entirely absent for **PmII** (i.e. **PyII** > **FPyII** > **PmII**).

Qualitatively, the correlation of this trend with decreasing Lewis basicities of the aromatic cores in these systems provides suggestions for the cause of this inhibitory behavior (Figure 16). Spectroscopic investigations prove that the substrate aldehyde is involved in dynamic association with the dialkylzinc reagent by coordination of the ring nitrogen (red equilibrium).<sup>64</sup> However, such a binding precludes the *floor-to-floor* association to the tetrameric catalyst, which is necessary for catalyst activity. Thus, it is hypothesized that inhibition results from competitive binding of the reagent to the substrate ring nitrogen, making the substrate unavailable for association to the O-Zn center in the catalyst. Consistent with observations, the extent of inhibition correlates with the strength of the N-

Zn association, which in turn must depend on the Lewis basicity of the azaaryl moieties. This hypothesis was further explored by reaction modeling of kinetic data to an autocatalytic mechanism and model simulations.

### 3.4. Insights from Kinetic Modeling – Steps Affecting Reaction Progression.

—On the basis of the mechanistic knowledge gained so far, a minimal set of elementary steps can be compiled for the definition of the autocatalytic reaction pathway (the *simplified floor-to-floor*–'SF' model, Figure 17). These steps are: (1) equilibrium binding of substrate aldehyde (A) and diisopropylzinc (Z) to yield the N-Zn bound adduct (AZ); (2) equilibrium binding of the catalyst (C) to diisopropylzinc (Z) at the pyridyl arm (binding by only one arm is considered for simplicity) to yield the active species (CZ); (3) equilibrium binding of substrate aldehyde (A) to the catalyst-diisopropylzinc adduct (AZ) to yield the activated complex (ACZ); (4) alkyl transfer from the SMS tetramer active complex (ACZ) to yield the catalyst-bound product alkoxide adduct (PC); (5) equilibrium dissociation of the product monomer alkoxide (P) to regenerate the SMS tetramer (C); (6) dimerization of the monomeric alkoxide (P) product to a dimeric unit (2P); and (7) dimerization of the dimeric unit (2P) to yield the newly constituted SMS tetramer (C). Rate constants for each step are designated. Arguably, this is a simplified picture of the actual catalytic process and additional steps can be envisaged. For example, the binding of two molecules of diisopropylzinc to the catalyst are ignored; the order of binding of the reagent and aldehyde to the SMS tetramer may be different than the one suggested here; reagent binding to the product alkoxide may exist; the precise mechanism of tetramer reformation is reasonable but nonetheless speculative; the contribution of an uncatalyzed background alkylation is ignored etc. However, the scheme incorporates all fundamental binding events necessary and sufficient to achieve compatibility with the 'SMS tetramer – floor to floor' (SF) autocatalysis model.

This model could qualitatively reproduce the autocatalytic reaction profiles for the **PyII** system, including the inhibitory effect of diisopropylzinc, and with chemically realistic kinetic parameters.<sup>65</sup> Model simulations reveal that among the seven proposed elementary steps, the rate of *reaction progression is sensitive only to the kinetic parameters of steps 1, 3 and 4* (Figure 17, red) in the following manner:<sup>65</sup> (1) decreasing the association constant  $K_{1a}$  results in faster reactions and decreasing extent of diisopropylzinc inhibition, mimicking the transitions from the **PyII** (to **FPyII**) to **PmII** systems (2) an increase in the value of  $K_{3a}$  results in faster reactions, and (3) an increase in the value of  $k_c$  results in faster reactions.

To a first approximation, the relative rates of the **PyII**, **FPyII** and **PmII** systems, and the differences in severity of diisopropylzinc inhibition originate from divergent contributions from the three autocatalytic-progression determining steps in the SF model (Figure 17). Considering the Lewis basicity of the aromatic nitrogen atoms, the  $K_{1a}$  values for the three systems are expected to be in the order: **PmII**  $\ll$  **FPyII**  $<$  **PyII**.<sup>68–70</sup> Moreover, the adduct for the pyrimidine system (red box) is in principle, a competent species because *floor-to-floor* binding is still feasible with the second pyrimidine nitrogen atom. The binding constant for reagent coordination to this second nitrogen (necessary to render the adduct incompetent) is expected to be very low. Taken together, these factors must contribute to a very low effective value of  $K_{1a}$  in the pyrimidine system, thus accounting for its

extraordinary rate and absence of inhibitory behavior (this is reproduced in the model simulations). *The qualitative prediction of  $K_{3a}$  and  $k_c$  is non trivial.* In the three systems, the Lewis basicity of the substrate nitrogen atoms and the Lewis acidities of the unsaturated tetramer zinc atoms follow opposite trends, thus confounding a comparative estimate of the association constant for step 3. Similarly, the nucleophilicity of the catalyst-arm bound diisopropylzinc molecule, and the electrophilicity of the bound substrate follow opposite trends in the three systems, which complicate a comparative estimate of the alkyl transfer rate constant. Ultimately, an interplay of contributions from these steps must dictate the overall trend of reaction progression. Kinetic simulations are consistent with this hypothesis; modifying the values of  $K_{1a}$ ,  $K_{3a}$  and  $k_c$  to mimic the three systems can indeed reproduce their relative rate profiles.<sup>65</sup> Taken together, these preliminary modeling studies reveal how the substrate-reagent binding equilibrium, catalyst-substrate binding equilibrium and the alkyl transfer rate contribute to: (1) rate of autocatalytic progression, (2) the origin of the extraordinarily rapid reactions in the **PmII** system, and (3) the origin of the relative extents of inhibition in the **PyII** and **FPyII** systems.

## CONCLUSIONS AND OUTLOOK

The strategy of *mixed catalyst-substrate* experiments allowed extensive study of structure activity relationships in the pyrimidine and pyridine systems. The results from these studies enabled a formulation of the roles played by structural constituents in effecting catalysis and selectivity in the Soai reaction. Contributions of the alkynyl substituent toward catalyst solubility, autocatalyst conformation, aggregate formation and enhancing substrate directed reactivity and enantioselectivity were elucidated. Similarly, subtle correlations of the alkyl groups and the aromatic core were identified.

An exploration of substituted nicotinaldehyde derivatives led to the determination of novel, competent substrates. Among these, the 5-fluoro-6-((trimethylsilyl)ethynyl)-nicotinaldehyde (**FPyII**) system provided an opportunity to carry out a careful comparison between three autocatalytic systems in regard to the Lewis basicity of the aromatic nitrogen. Model kinetic simulations revealed how this factor critically influences the interplay of three steps in the autocatalytic pathway that are determinants of reaction progression. The low Lewis basicity of the pyrimidine nitrogen abrogates inhibition effects and results in superlative performance in the Soai reaction. These structural insights are completely consistent with the *floor-to-floor* transition state model presented earlier.<sup>64</sup>

The mechanistic landscape of the Soai reaction can now be summarized as follows: (1) the diisopropylzinc alkylation of Soai substrates affords isopropylzinc alkoxides that can access the SMS-tetramer by a combination of steric effects and nitrogen coordination (cube-escape model); (2) in general, this tetramer can enantioselectively alkylate a variety of aldehydes that belong to the pyridine-3-carbaldehyde scaffold (which includes pyrimidine-5-carbaldehydes) via a two-point *floor-to-floor* model — an autocatalytic reaction is simply a special case occurring for a ‘matched’ substrate; (3) structural effects play a critical role in the assembly of the SMS tetramer, its solubility, active conformation and substrate accessibility as well as the reactivity and selectivity imparted by the substrate — the rationalization of these effects largely explains the idiosyncratic substrate scope of this



transformation; (4) reaction progression is dictated by the strength of N-Zn binding events – some of which are inhibitory — the low Lewis basicity of the pyrimidine nitrogen allows this system to overcome such inhibitory effects and attain superior autocatalytic rates; and (5) the striking non-linear behavior of the reaction is attributed to the poor catalytic competence of the heterochiral SMS tetramer that cannot engage the substrate in the *floor-to-floor* binding mode.

The precise manner in which the autocatalytic cycle is completed (dissociation of the product alkoxide and its re-assembly into the SMS tetramer) remains to be elucidated. Likewise, for a scalemic SMS tetramer, multiple interconverting isomeric forms (due to alternative configurations of the chiral, tetracoordinate alkoxyzinc atoms) are theoretically possible. A rigorous study on the distribution and relative catalytic activities of these isomers, has not yet been performed. In our opinion, these outstanding investigations, anticipated to be predominantly computational in enquiry, will provide further mechanistic understanding of the remarkable Soai reaction.

## Supplementary Material

Refer to Web version on PubMed Central for supplementary material.

## ACKNOWLEDGEMENTS

We are grateful for generous financial support from the University of Illinois. S.V.A. is grateful to the University of Illinois for Graduate Fellowships. A.S. thanks the NIH Chemistry-Biology Interface Research Training Grant (T32GM008496). We are also grateful for the support services of the NMR, mass spectrometry and microanalytical laboratories of the University of Illinois at Urbana-Champaign.

## REFERENCES

- (1). Soai K; Shibata T; Morioka H; Choji K Asymmetric Autocatalysis and Amplification of Enantiomeric Excess of a Chiral Molecule. *Nature* 1995, 378 (6559), 767–768.
- (2). Although the active catalyst is certainly derived from the in-situ generated zinc alkoxide, the term ‘catalyst’, for simplicity throughout this thesis, is used interchangeably for the carbinol or the alkoxide. Similarly, the term ‘product’ is used interchangeably for the product zinc alkoxide or the product carbinol obtained after workup.
- (3). Shibata T; Morioka H; Hayase T; Choji K; Soai K Highly Enantioselective Catalytic Asymmetric Automultiplication of Chiral Pyrimidyl Alcohol. *J. Am. Chem. Soc* 1996, 118 (2), 471–472.
- (4). Shibata T; Yonekubo S; Soai K Practically Perfect Asymmetric Autocatalysis with (2-Alkynyl-5-Pyrimidyl)Alkanols. *Angew. Chem. Int. Ed* 1999, 38 (5), 659–661.
- (5). Sato I; Yanagi T; Soai K Highly Enantioselective Asymmetric Autocatalysis of 2-Alkenyl- and 2-Vinyl-5-Pyrimidyl Alkanols with Significant Amplification of Enantiomeric Excess. *Chirality* 2002, 14 (2–3), 166–168. [PubMed: 11835560]
- (6). Lutz F; Kawasaki T; Soai K Asymmetric Autocatalysis of a Ferrocene-Containing Chiral Compound with Amplification of Chirality. *Tetrahedron Asymmetry* 2006, 17 (4), 486–490.
- (7). Busch M; Schlageter M; Weingand D; Gehring T Systematic Studies Using 2-(1-Adamantylethynyl)Pyrimidine-5-Carbaldehyde as a Starting Material in Soai’s Asymmetric Autocatalysis. *Chem. – Eur. J* 2009, 15 (33), 8251–8258. [PubMed: 19585641]
- (8). Kawasaki T; Kamimura S; Amihara A; Suzuki K; Soai K Enantioselective C-C Bond Formation as a Result of the Oriented Prochirality of an Achiral Aldehyde at the Single-Crystal Face upon Treatment with a Dialkyl Zinc Vapor. *Angew. Chem. Int. Ed* 2011, 50 (30), 6796–6798.

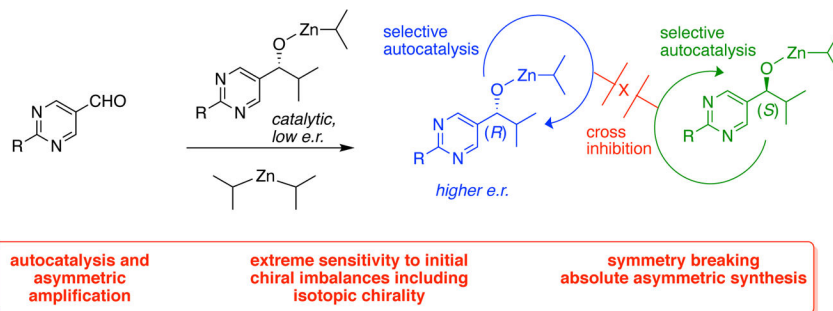
- (9). Frank FC On Spontaneous Asymmetric Synthesis. *Biochim. Biophys. Acta* 1953, 11, 459–463. [PubMed: 13105666]
- (10). Wynberg H Asymmetric Autocatalysis: Facts and Fancy. *J. Macromol. Sci. Part - Chem* 1989, 26 (8), 1033–1041.
- (11). Sato I; Urabe H; Ishiguro S; Shibata T; Soai K Amplification of Chirality from Extremely Low to Greater than 99.5 % ee by Asymmetric Autocatalysis. *Angew. Chem. Int. Ed* 2003, 42 (3), 315–317.
- (12). Soai K; Shibata T; Kowata Y: Japan Kokai Tokkyo Koho JP 1997 9–268179. Application Date: February 1 and April 18, 1996.
- (13). Soai K; Sato I; Shibata T; Komiya S; Hayashi M; Matsueda Y; Imamura H; Hayase T; Morioka H; Tabira H; Yamamoto J; Kowata Y Asymmetric Synthesis of Pyrimidyl Alkanol without Adding Chiral Substances by the Addition of Diisopropylzinc to Pyrimidine-5-Carbaldehyde in Conjunction with Asymmetric Autocatalysis. *Tetrahedron Asymmetry* 2003, 14 (2), 185–188.
- (14). Kaimori Y; Hiyoshi Y; Kawasaki T; Matsumoto A; Soai K Formation of Enantioenriched Alkanol with Stochastic Distribution of Enantiomers in the Absolute Asymmetric Synthesis under Heterogeneous Solid–Vapor Phase Conditions. *Chem. Commun* 2019, 55 (36), 5223–5226.
- (15). Singleton DA; Vo LK Enantioselective Synthesis without Discrete Optically Active Additives. *J. Am. Chem. Soc* 2002, 124 (34), 10010–10011. [PubMed: 12188664]
- (16). Singleton DA; Vo LK A Few Molecules Can Control the Enantiomeric Outcome. Evidence Supporting Absolute Asymmetric Synthesis Using the Soai Asymmetric Autocatalysis. *Org. Lett* 2003, 5 (23), 4337–4339. [PubMed: 14601994]
- (17). Mislow K Absolute Asymmetric Synthesis: A Commentary. *Collect. Czech. Chem. Commun* 2003, 68, 849–864.
- (18). Sato I; Ohgo Y; Igarashi H; Nishiyama D; Kawasaki T; Soai K Determination of Absolute Configurations of Amino Acids by Asymmetric Autocatalysis of 2-Alkynylpyrimidyl Alkanol as a Chiral Sensor. *J. Organomet. Chem* 2007, 692 (9), 1783–1787.
- (19). Kawasaki T; Jo K; Igarashi H; Sato I; Nagano M; Koshima H; Soai K Asymmetric Amplification Using Chiral Cocrystals Formed from Achiral Organic Molecules by Asymmetric Autocatalysis. *Angew. Chem. Int. Ed* 2005, 44 (18), 2774–2777.
- (20). Sato I; Yamashima R; Kadowaki K; Yamamoto J; Shibata T; Soai K Asymmetric Induction by Helical Hydrocarbons: [6]- and [5]Helicenes. *Angew. Chem. Int. Ed* 2001, 40 (6), 1096–1098.
- (21). Kawasaki T; Tanaka H; Tsutsumi T; Kasahara T; Sato I; Soai K Chiral Discrimination of Cryptochiral Saturated Quaternary and Tertiary Hydrocarbons by Asymmetric Autocatalysis. *J. Am. Chem. Soc* 2006, 128 (18), 6032–6033. [PubMed: 16669661]
- (22). Soai K; Kawasaki T; Matsumoto A Asymmetric Autocatalysis of Pyrimidyl Alkanol and Its Application to the Study on the Origin of Homochirality. *Acc. Chem. Res* 2014, 47 (12), 3643–3654. [PubMed: 25511374]
- (23). Kawasaki T; Sato M; Ishiguro S; Saito T; Morishita Y; Sato I; Nishino H; Inoue Y; Soai K Enantioselective Synthesis of Near Enantiopure Compound by Asymmetric Autocatalysis Triggered by Asymmetric Photolysis with Circularly Polarized Light. *J. Am. Chem. Soc* 2005, 127 (10), 3274–3275. [PubMed: 15755133]
- (24). Kawasaki T; Matsumura Y; Tsutsumi T; Suzuki K; Ito M; Soai K Asymmetric Autocatalysis Triggered by Carbon Isotope ( $^{13}\text{C}/^{12}\text{C}$ ) Chirality. *Science* 2009, 324 (5926), 492–495. [PubMed: 19325079]
- (25). Kawasaki T; Okano Y; Suzuki E; Takano S; Oji S; Soai K Asymmetric Autocatalysis: Triggered by Chiral Isotopomer Arising from Oxygen Isotope Substitution. *Angew. Chem. Int. Ed* 2011, 50 (35), 8131–8133.
- (26). Matsumoto A; Ozaki H; Harada S; Tada K; Ayugase T; Ozawa H; Kawasaki T; Soai K Asymmetric Induction by a Nitrogen  $^{14}\text{N}/^{15}\text{N}$  Isotopomer in Conjunction with Asymmetric Autocatalysis. *Angew. Chem. Int. Ed* 2016, 55, 15246–15249.
- (27). Blackmond DG The Origin of Biological Homochirality. *Cold Spring Harb. Perspect. Biol* 2010, 2 (5), a002147. [PubMed: 20452962]
- (28). Rolf M Flügel Chirality and Life: A Short Introduction to the Early Phases of Chemical Evolution, 1st ed.; Springer-Verlag Berlin Heidelberg, 2011.

- (29). Weissbuch I; Lahav M Crystalline Architectures as Templates of Relevance to the Origins of Homochirality. *Chem. Rev* 2011, 111 (5), 3236–3267. [PubMed: 21381662]
- (30). Cintas P *Biochirality: Origins, Evolution and Molecular Recognition.*, 1st ed.; Pedro Cintas, Ed.; Topics in Current Chemistry; Springer-Verlag Berlin Heidelberg, 2013.
- (31). Barabás B; Fülöp O, Chapter 3 - Graph Theoretical and Statistical Analysis of the Impact of Soai Reaction on Natural Sciences, in *Advances in Asymmetric Autocatalysis and Related Topics*. Ed. Palyi G; Kurdi R; Zucchi C, Academic Press, 2017.
- (32). Gehring T; Busch M; Schlageter M; Weingand D A Concise Summary of Experimental Facts about the Soai Reaction. *Chirality* 2010, 22 (1E), E173–E182. [PubMed: 21038388]
- (33). Soai K; Matsumoto A; Kawasaki T, Chapter 1 - Asymmetric Autocatalysis and the Origins of Homochirality of Organic Compounds, in *Advances in Asymmetric Autocatalysis and Related Topics*. Ed. Palyi G; Kurdi R; Zucchi C, Academic Press, 2017.
- (34). Buhse T; Noble-Terán ME; Cruz J-M; Micheau J-C; Coudret C, Chapter 4 - Kinetic and Structural Aspects of Mirror-Image Symmetry Breaking in the Soai Reaction, in *Advances in Asymmetric Autocatalysis and Related Topics*. Ed. Palyi G; Kurdi R; Zucchi C, Academic Press, 2017.
- (35). Blackmond DG Autocatalytic Models for the Origin of Biological Homochirality. *Chem. Rev* 2019, acs.chemrev.9b00557.
- (36). Soai K; Niwa S; Hori H Asymmetric Self-Catalytic Reaction. Self-Production of Chiral 1-(3-Pyridyl)Alkanols as Chiral Self-Catalysts in the Enantioselective Addition of Dialkylzinc Reagents to Pyridine-3-Carbaldehyde. *J. Chem. Soc. Chem. Commun* 1990, No. 14, 982–983.
- (37). Klankermayer J; Gridnev ID; Brown JM Role of the Isopropyl Group in Asymmetric Autocatalytic Zinc Alkylations. *Chem. Commun* 2007, No. 30, 3151–3153.
- (38). Gridnev ID; Serafimov JM; Quiney H; Brown JM Reflections on Spontaneous Asymmetric Synthesis by Amplifying Autocatalysis. *Org. Biomol. Chem* 2003, 1 (21), 3811–3819. [PubMed: 14649913]
- (39). Shibata T; Choji K; Hayase T; Aizu Y; Soai K Asymmetric Autocatalytic Reaction of 3-Quinolylalkanol with Amplification of Enantiomeric Excess. *Chem. Commun* 1996, No. 10, 1235–1236.
- (40). Shibata T; Choji K; Morioka H; Hayase T; Soai K Highly Enantioselective Synthesis of a Chiral 3-Quinolylalkanol by an Asymmetric Autocatalytic Reaction. *Chem. Commun* 1996, No. 6, 751–752.
- (41). Sato I; Nakao T; Sugie R; Kawasaki T; Soai K Enantioselective Synthesis of Substituted 3-Quinolyl Alkanols and Their Application to Asymmetric Autocatalysis. *Synthesis* 2004, 9, 1419–1428.
- (42). Tanji S; Kodaka Y; Ohno A; Shibata T; Sato I; Soai K Asymmetric Autocatalysis of 5-Carbamoyl-3-Pyridyl Alkanols with Amplification of Enantiomeric Excess. *Tetrahedron Asymmetry* 2000, 11 (21), 4249–4253.
- (43). Hawbaker NA; Blackmond DG Rationalization of Asymmetric Amplification via Autocatalysis Triggered by Isotopically Chiral Molecules. *ACS Cent. Sci* 2018, 4 (6), 776–780. [PubMed: 29974074]
- (44). Hawbaker NA; Blackmond DG Energy Threshold for Chiral Symmetry Breaking in Molecular Self-Replication. *Nat. Chem* 2019, 11 (10), 957–962. [PubMed: 31548669]
- (45). Blackmond DG; McMillan CR; Ramdeehul S; Schorm A; Brown JM Origins of Asymmetric Amplification in Autocatalytic Alkylzinc Additions. *J. Am. Chem. Soc* 2001, 123 (41), 10103–10104. [PubMed: 11592892]
- (46). Buhse Thomas. A Tentative Kinetic Model for Chiral Amplification in Autocatalytic Alkylzinc Additions. *Asymmetry* 2003, 14, 1055–1061.
- (47). Sato I; Omiya D; Igarashi H; Kato K; Ogi Y; Tsukiyama K; Soai K Relationship between the Time, Yield, and Enantiomeric Excess of Asymmetric Autocatalysis of Chiral 2-Alkynyl-5-Pyrimidyl Alkanol with Amplification of Enantiomeric Excess. *Tetrahedron Asymmetry* 2003, 14 (8), 975–979.

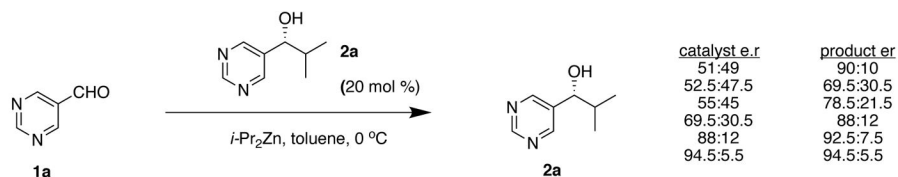
- (48). Buono FG; Blackmond DG Kinetic Evidence for a Tetrameric Transition State in the Asymmetric Autocatalytic Alkylation of Pyrimidyl Aldehydes. *J. Am. Chem. Soc* 2003, 125 (30), 8978–8979. [PubMed: 15369330]
- (49). Gridnev ID; Serafimov JM; Brown JM Solution Structure and Reagent Binding of the Zinc Alkoxide Catalyst in the Soai Asymmetric Autocatalytic Reaction. *Angew. Chem. Int. Ed* 2004, 43 (37), 4884–4887.
- (50). Brown JM; Gridnev I; Klankermayer J Asymmetric Autocatalysis with Organozinc Complexes; Elucidation of the Reaction Pathway In Amplification of Chirality; Soai K, Ed.; Springer Berlin Heidelberg: Berlin, Heidelberg, 2008; pp 35–65.
- (51). Islas JR; Lavabre D; Grevy J-M; Lamonedá RH; Cabrera HR; Micheau J-C; Buhse T Mirror-Symmetry Breaking in the Soai Reaction: A Kinetic Understanding. *Proc. Natl. Acad. Sci. U. S. A* 2005, 102 (39), 13743–13748. [PubMed: 16174731]
- (52). Micskei K; Póta G; Caglioti L; Pályi G Empirical Description of Chiral Autocatalysis. *J. Phys. Chem. A* 2006, 110 (18), 5982–5984. [PubMed: 16671665]
- (53). Schiaffino L; Ercolani G Unraveling the Mechanism of the Soai Asymmetric Autocatalytic Reaction by First-Principles Calculations: Induction and Amplification of Chirality by Self-Assembly of Hexamolecular Complexes. *Angew. Chem. Int. Ed* 2008, 47 (36), 6832–6835.
- (54). Micskei K; Rábai G; Gál E; Caglioti L; Pályi G Oscillatory Symmetry Breaking in the Soai Reaction. *J. Phys. Chem. B* 2008, 112 (30), 9196–9200. [PubMed: 18593153]
- (55). Schiaffino L; Ercolani G Amplification of Chirality and Enantioselectivity in the Asymmetric Autocatalytic Soai Reaction. *ChemPhysChem* 2009, 10 (14), 2508–2515. [PubMed: 19708050]
- (56). Micheau J-C; Cruz J-M; Coudret C; Buhse T An Autocatalytic Cycle Model of Asymmetric Amplification and Mirror-Symmetry Breaking in the Soai Reaction. *ChemPhysChem* 2010, 11 (16), 3417–3419. [PubMed: 20922741]
- (57). Quaranta M; Gehring T; Odell B; Brown JM; Blackmond DG Unusual Inverse Temperature Dependence on Reaction Rate in the Asymmetric Autocatalytic Alkylation of Pyrimidyl Aldehydes. *J. Am. Chem. Soc* 2010, 132 (43), 15104–15107. [PubMed: 20942400]
- (58). Ercolani G; Schiaffino L Putting the Mechanism of the Soai Reaction to the Test: DFT Study of the Role of Aldehyde and Dialkylzinc Structure. *J. Org. Chem* 2011, 76 (8), 2619–2626. [PubMed: 21401089]
- (59). Gridnev ID; Vorobiev AK Quantification of Sophisticated Equilibria in the Reaction Pool and Amplifying Catalytic Cycle of the Soai Reaction. *ACS Catal.* 2012, 2 (10), 2137–2149.
- (60). Matsumoto A; Abe T; Hara A; Tobita T; Sasagawa T; Kawasaki T; Soai K Crystal Structure of the Isopropylzinc Alkoxide of Pyrimidyl Alkanol: Mechanistic Insights for Asymmetric Autocatalysis with Amplification of Enantiomeric Excess. *Angew. Chem. Int. Ed* 2015, 54 (50), 15218–15221.
- (61). Matsumoto A; Kawasaki T; Soai K, Chapter 10 - Structural Study of Asymmetric Autocatalysis by X-Ray Crystallography, in *Advances in Asymmetric Autocatalysis and Related Topics*. Ed. Pályi G; Kurdi R; Zucchi C, Academic Press, 2017.
- (62). Gridnev ID; Brown JM Asymmetric Catalysis Special Feature Part II: Asymmetric Autocatalysis: Novel Structures, Novel Mechanism? *Proc. Natl. Acad. Sci* 2004, 101 (16), 5727–5731. [PubMed: 15060283]
- (63). Matsumoto A; Fujiwara S; Abe T; Hara A; Tobita T; Sasagawa T; Kawasaki T; Soai K Elucidation of the Structures of Asymmetric Autocatalyst Based on X-Ray Crystallography. *Bull. Chem. Soc. Jpn* 2016, 89 (10), 1170–1177.
- (64). Athavale SV; Simon A; Houk KN; Denmark SE Demystifying the Asymmetry-Amplifying, Autocatalytic Behaviour of the Soai Reaction through Structural, Mechanistic and Computational Studies. *Nat. Chem* 2020, 12 (4), 412–423. [PubMed: 32203445]
- (65). Refer to Supplementary Information.
- (66). Krasovskiy A; Krasovskaya V; Knochel P Mixed Mg/Li Amides of the Type R<sub>2</sub>NMgCl-LiCl as Highly Efficient Bases for the Regioselective Generation of Functionalized Aryl and Heteroaryl Magnesium Compounds. *Angew. Chem. Int. Ed* 2006,

- (67). Romagnoli C; Sieng B; Amedjkouh M Asymmetric Amplification Coupling Enantioselective Autocatalysis and Asymmetric Induction for Alkylation of Azaaryl Aldehydes. *Eur. J. Org. Chem* 2015, 2015 (19), 4087–4092.
- (68). Albert A; Goldacre R; Phillips J 455. The Strength of Heterocyclic Bases. *J. Chem. Soc. Resumed* 1948, 2240–2249.
- (69). Laurence C; Gal J-F; Lewis Basicity and Affinity Scales: Data and Measurement, John Wiley & Sons Ltd, 2010.
- (70). Clarke K; Rothwell K 377. A Kinetic Study of the Effect of Substituents on the Rate of Formation of Alkylpyridinium Halides in Nitromethane Solution. *J. Chem. Soc. Resumed* 1960, 1885.

a. Overall scheme for the amplifying autocatalytic Soai reaction



b. Seminal report (Soai, 1995)



Note: analogous reaction with pyridine-3-carbaldehyde (**3a**) shows poor asymmetric autocatalysis, with asymmetric erosion (Soai, 1990)

c. Improved Substrates: 2-alkynyl pyrimidine carbaldehydes

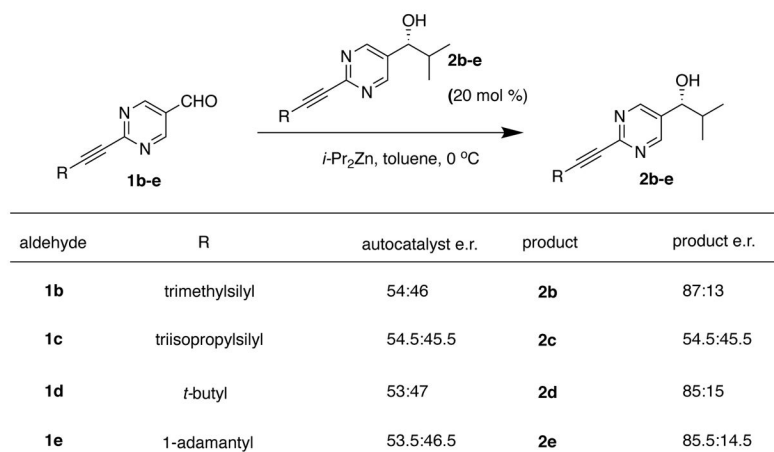


**Figure 1.**

(a) The Soai reaction, with the general scheme of amplifying autocatalysis and salient features. (b) Seminal report with substrate **1a**. (c) Improved performance with alkynyl substituted substrates, except in the case of **1c**.

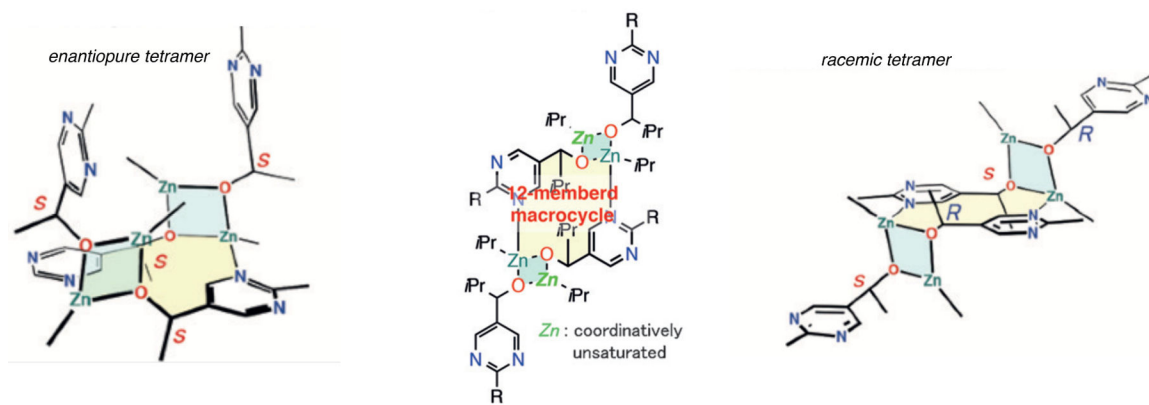


**Figure 2.**  
Crystal structures for the square-macrocycle-square (SMS) tetrameric isopropylzinc alkoxide derived from **2d**.

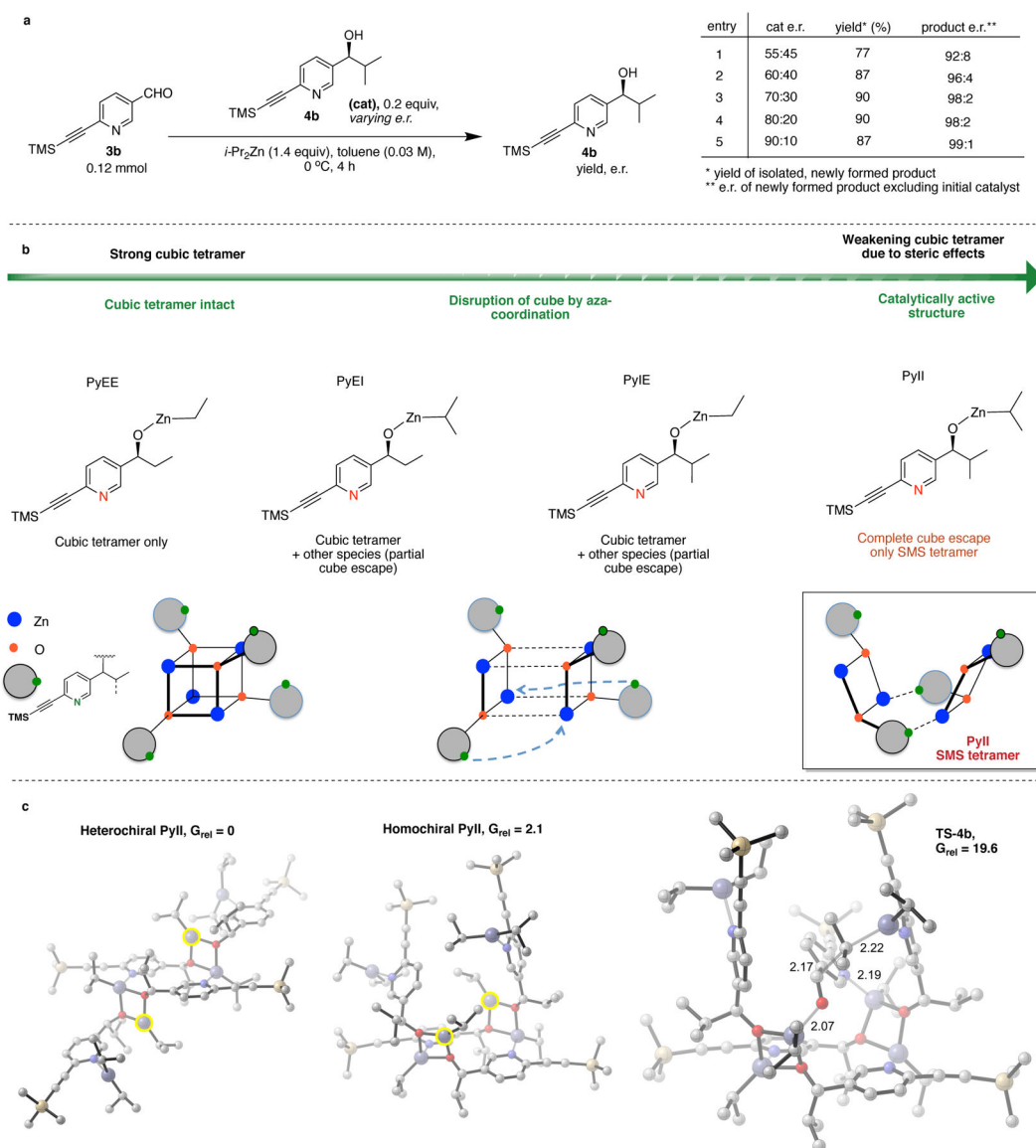


**Figure 3.** (a) Amplifying autocatalysis with substrate **3b**. (b) The cube escape model to rationalize the formation of the (auto)catalytically competent SMS tetramer. (c) (from left) DFT calculated structures and relative energies (kcal/mol) for the ground-state heterochiral and homochiral SMS tetramers. The stereo-determining, transition state structure on the right arises after a *floor-to-floor* binding of the substrate aldehyde **3b** to the homochiral tetramer. The location of the concerned zinc centers (yellow) in the heterochiral tetramer precludes such a binding mode.



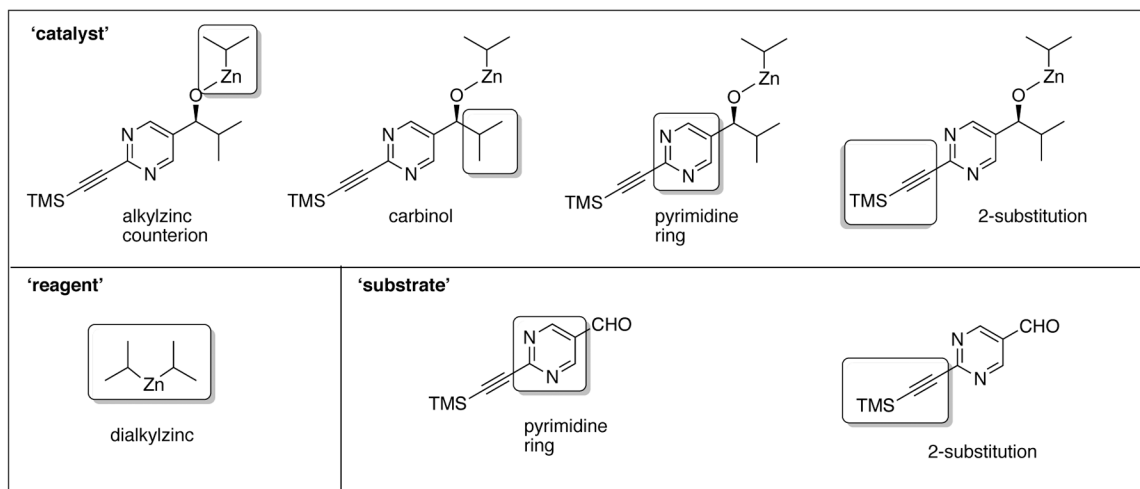
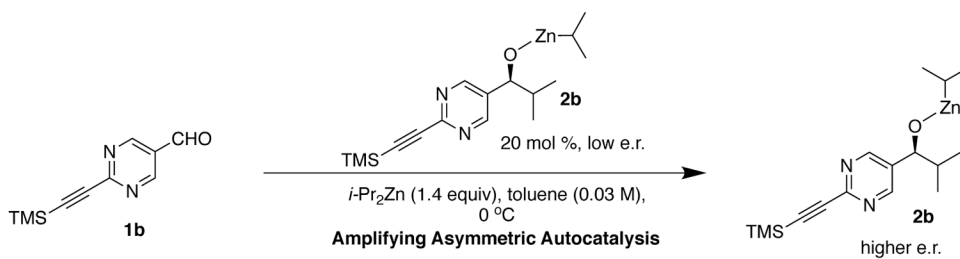
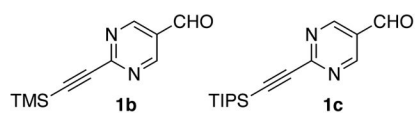


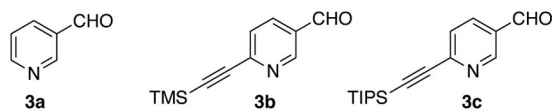
**Figure 4.** Structural constituents of the three components (catalyst, reagent and substrate) in the Soai reaction.

## Pyrimidine aldehydes



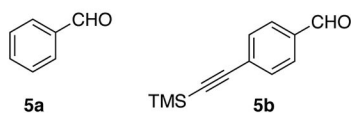
alkylation products: 2b-2c

## Pyridine aldehydes



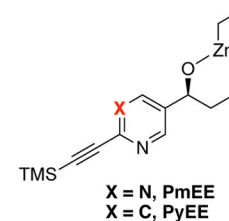
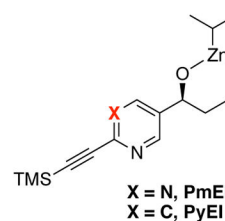
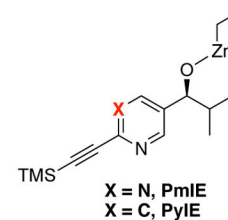
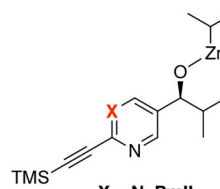
alkylation products: 3b-3c

## Benzaldehydes



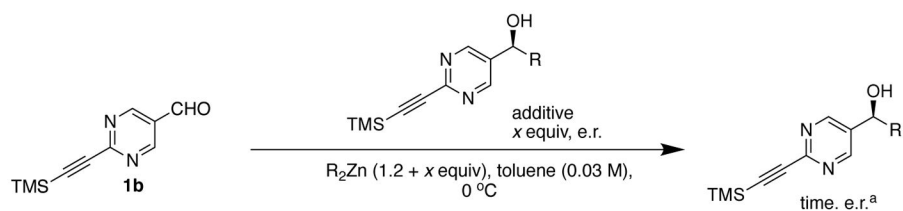
alkylation products: 6a-6b

## Zinc Alkoxides (catalysts)

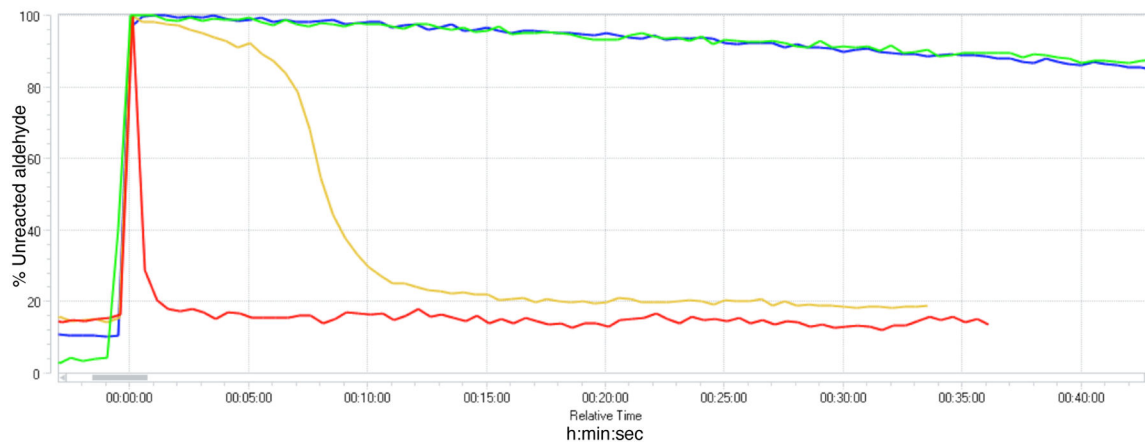


Guide:  
Pm/Py = pyrimidine/pyridine  
I = isopropyl  
E = ethyl

**Figure 5.**  
Compound numbering for substrates and zinc alkoxide catalysts.

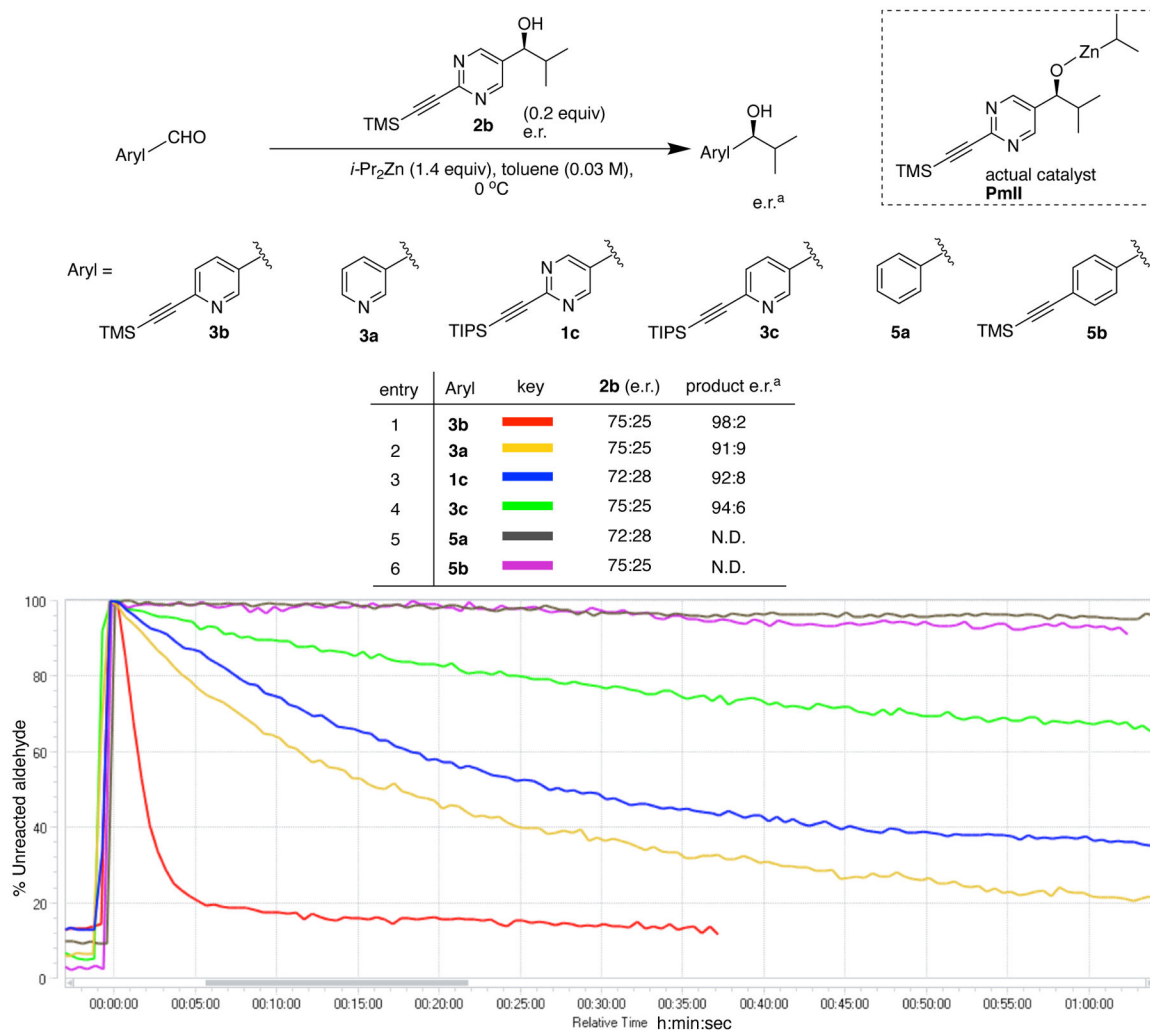


entry	R	x	e.r.	key	time (min)	product e.r. <sup>a</sup>	description
1	<i>i</i> -Pr	0	-		33	49:51	<i>i</i> -Pr <sub>2</sub> Zn, no cat
2	<i>i</i> -Pr	0.2	74:26		37	94:6 <sup>b</sup>	<i>i</i> -Pr <sub>2</sub> Zn, scalemic cat
3	Et	0	-		180	50:50	Et <sub>2</sub> Zn, no cat
4	Et	0.2	70:30		127	67:33 <sup>b</sup>	Et <sub>2</sub> Zn, scalemic cat



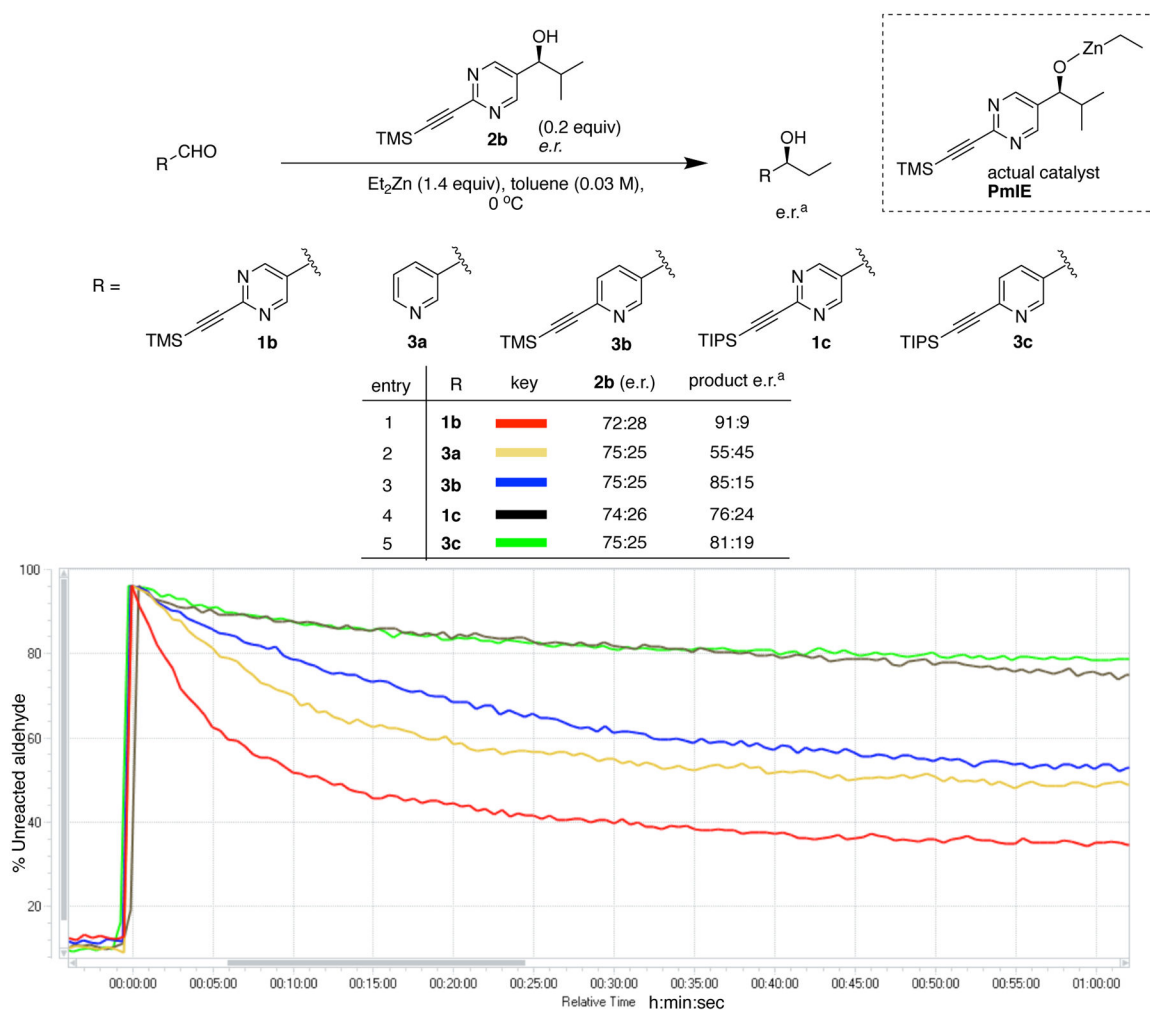
<sup>a</sup> Measured e.r. of the product carbinol after workup at indicated time <sup>b</sup> Measured e.r. which includes initially added catalyst

**Figure 6.**  
*In-situ* IR spectroscopic monitoring of the Soai reaction (wavenumber at  $\sim 1710\text{ cm}^{-1}$ ).



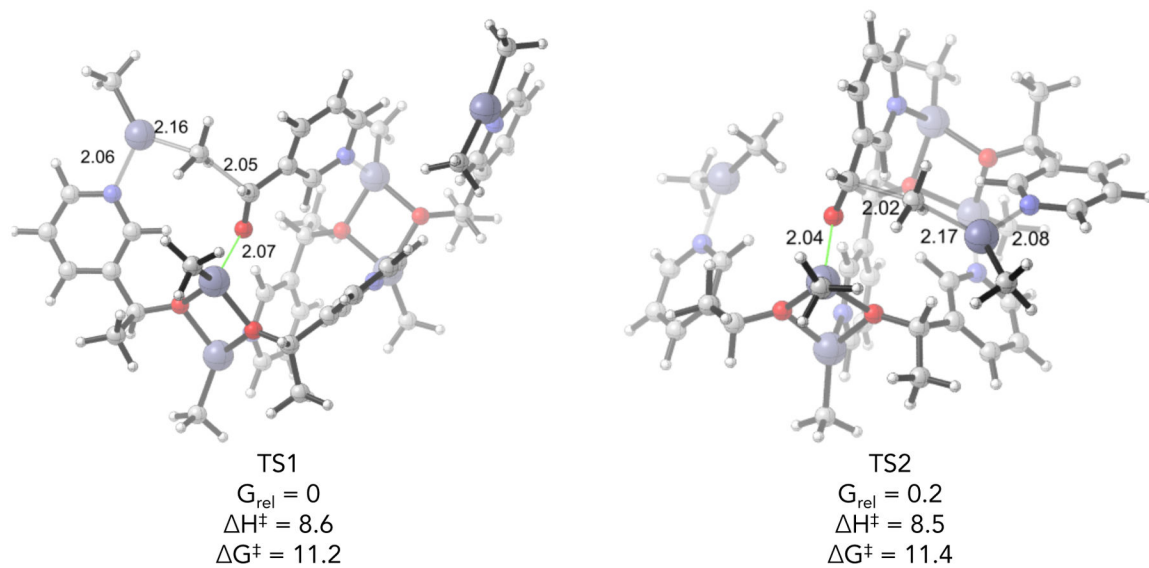
<sup>a</sup> Measured e.r. of product carbinol after workup, N.D. Not determined (no product was detected in these cases)

**Figure 7.** **PmII** catalyzed, 'mixed-catalyst substrate' diisopropylzinc alkylations monitored by *in-situ* IR spectroscopy.

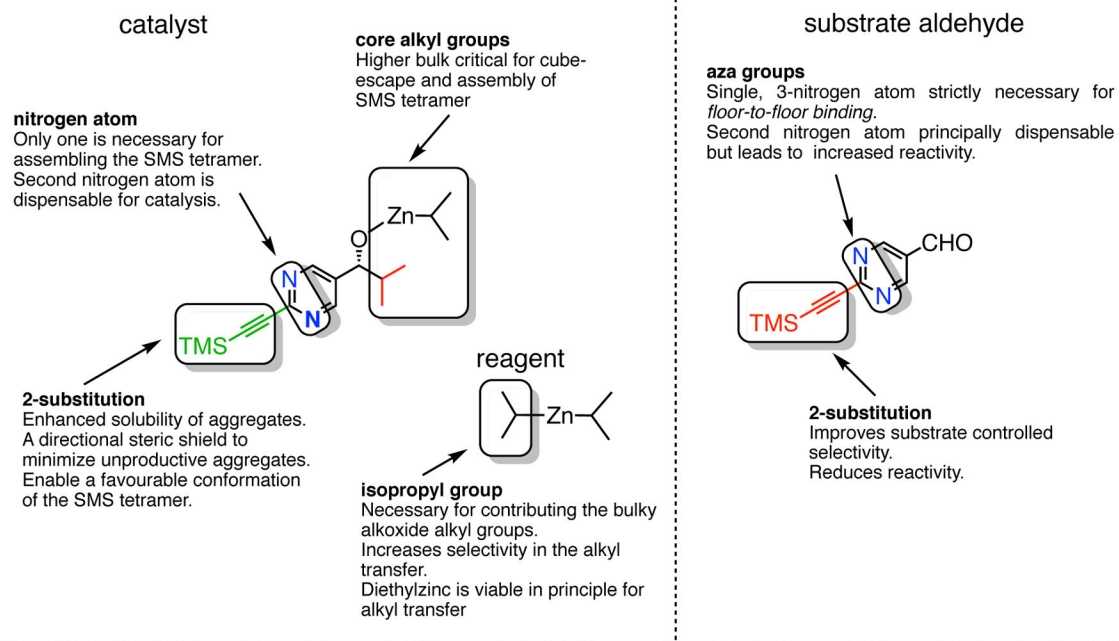


<sup>a</sup> Measured e.r. of the product carbinol after workup at indicated time

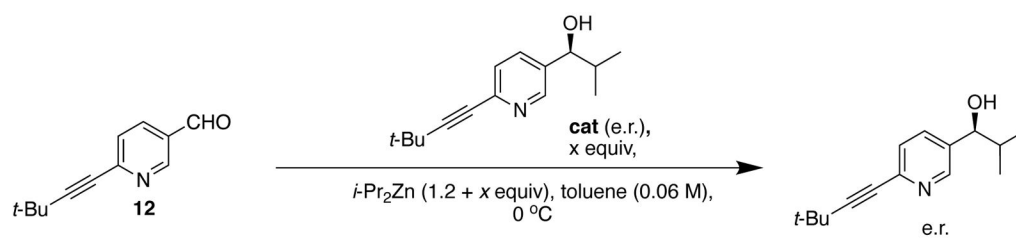
**Figure 8.** **PmIE** catalyzed ‘mixed-catalyst substrate’ diethylzinc alkylations monitored by *in-situ* IR spectroscopy.





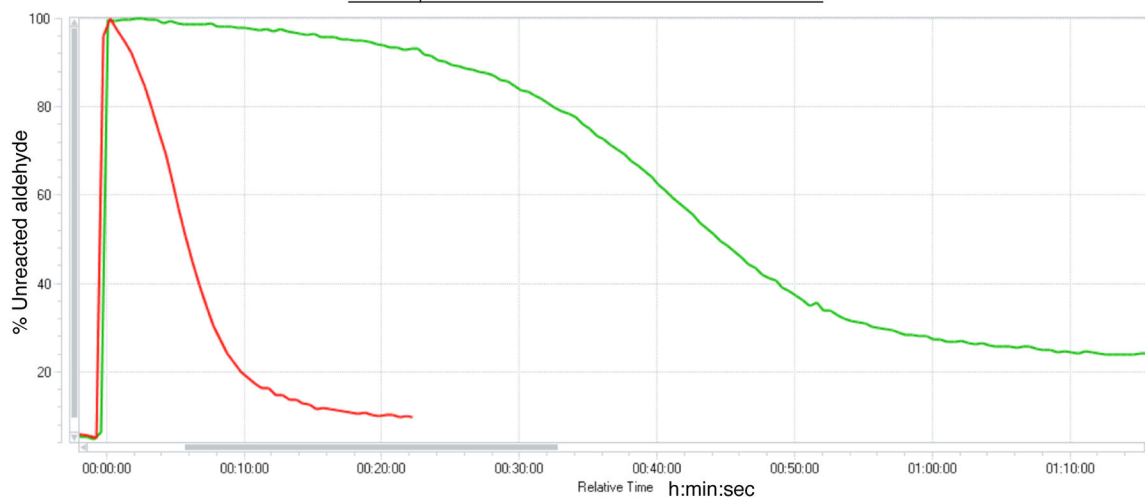
**Figure 9.** Transition state structures for **NII** catalyzed alkyl transfer to **3a**. Calculated at the M06-2X/def2-TZVPP-SMD (toluene)//B3LYP/6-31G(d) level of theory. Relative energies reported in kcal/mol. Purple, zinc; yellow, silicon; red, oxygen; blue, nitrogen; gray, carbon. Hydrogens are hidden for clarity.

**Figure 10:**

A summary of the roles played by various structural constituents in effecting catalysis and selectivity in the Soai system.



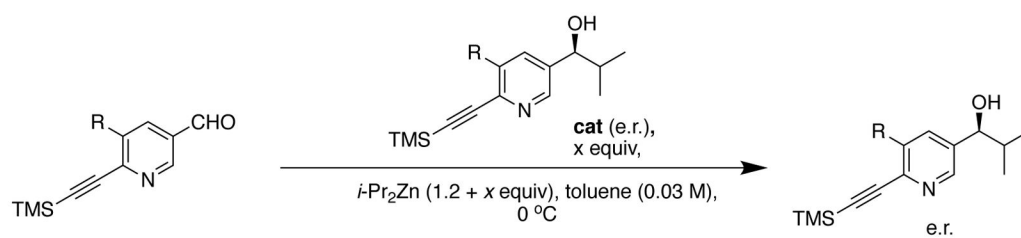
entry	$x$	cat (e.r.)	key	product e.r.
1	0	-		-
2	0.2	71:29		91:9 <sup>a</sup>









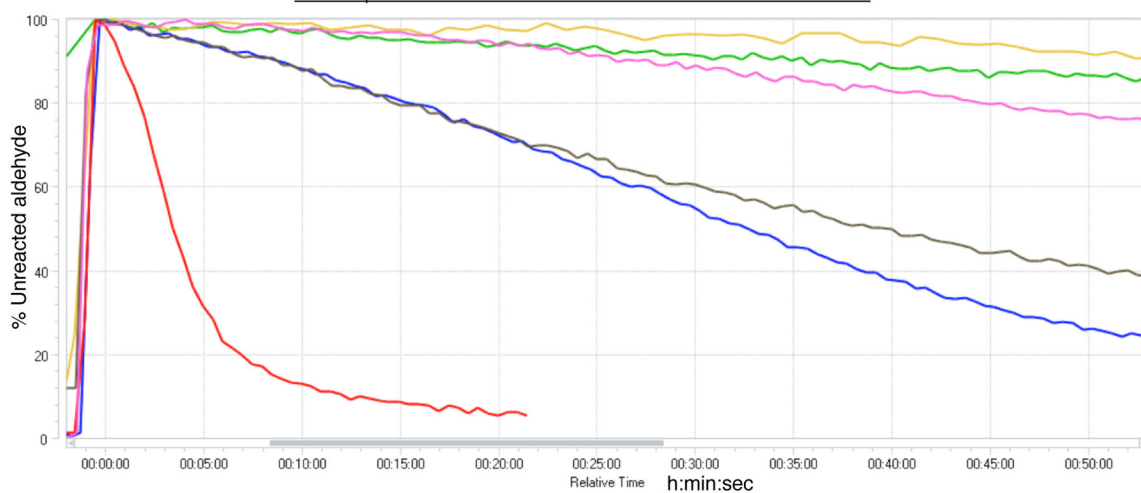
<sup>a</sup> Measured e.r. which includes initially added catalyst

**Figure 11.**  
Amplifying asymmetric autocatalysis in the reaction of **12** with diisopropylzinc.



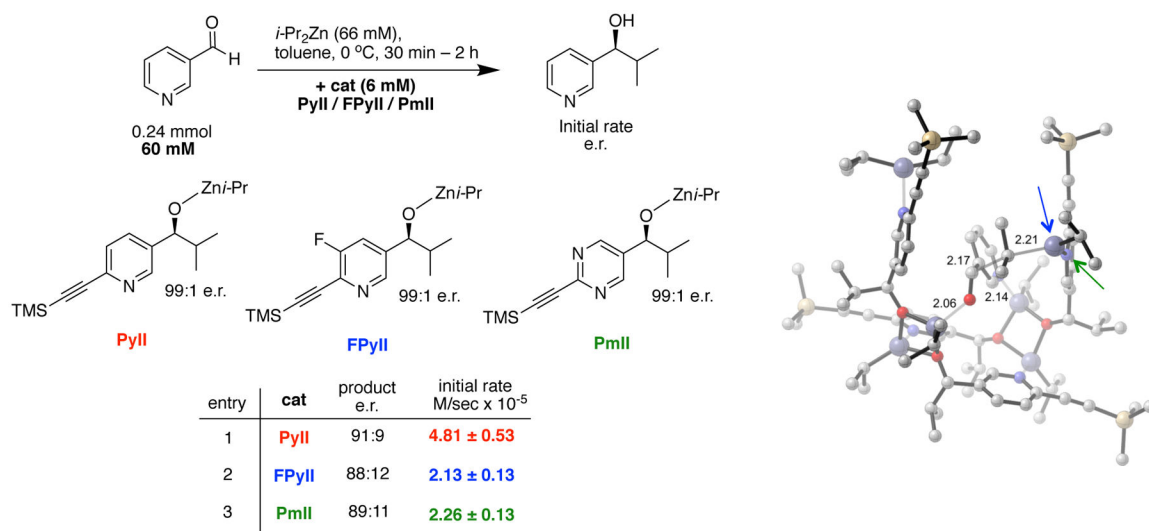


entry	R	x	cat (e.r.)	key	product e.r. <sup>a</sup>
1	Br ( <b>16</b> )	0	-		-
2	Br ( <b>16</b> )	0.2	72:28		80:20
3	Me ( <b>18</b> )	0	-		-
4	Me ( <b>18</b> )	0.2	66:34		85:15
5	F ( <b>19</b> )	0	-		-
6	F ( <b>19</b> )	0.2	71:28		93:7



<sup>a</sup> Measured e.r. which includes initially added catalyst

**Figure 12.**  
Amplifying asymmetric autocatalysis in the reaction of 5,6-disubstituted nicotinaldehyde with diisopropylzinc.

**Figure 13.**

Comparison of alkyl transfer rates of **PyII**, **FPyII** and **PmII**. TS model for the alkyl transfer with **PyII** highlighting the transferring diisopropylzinc moiety (blue arrow) bound to the activating arm nitrogen (green arrow).

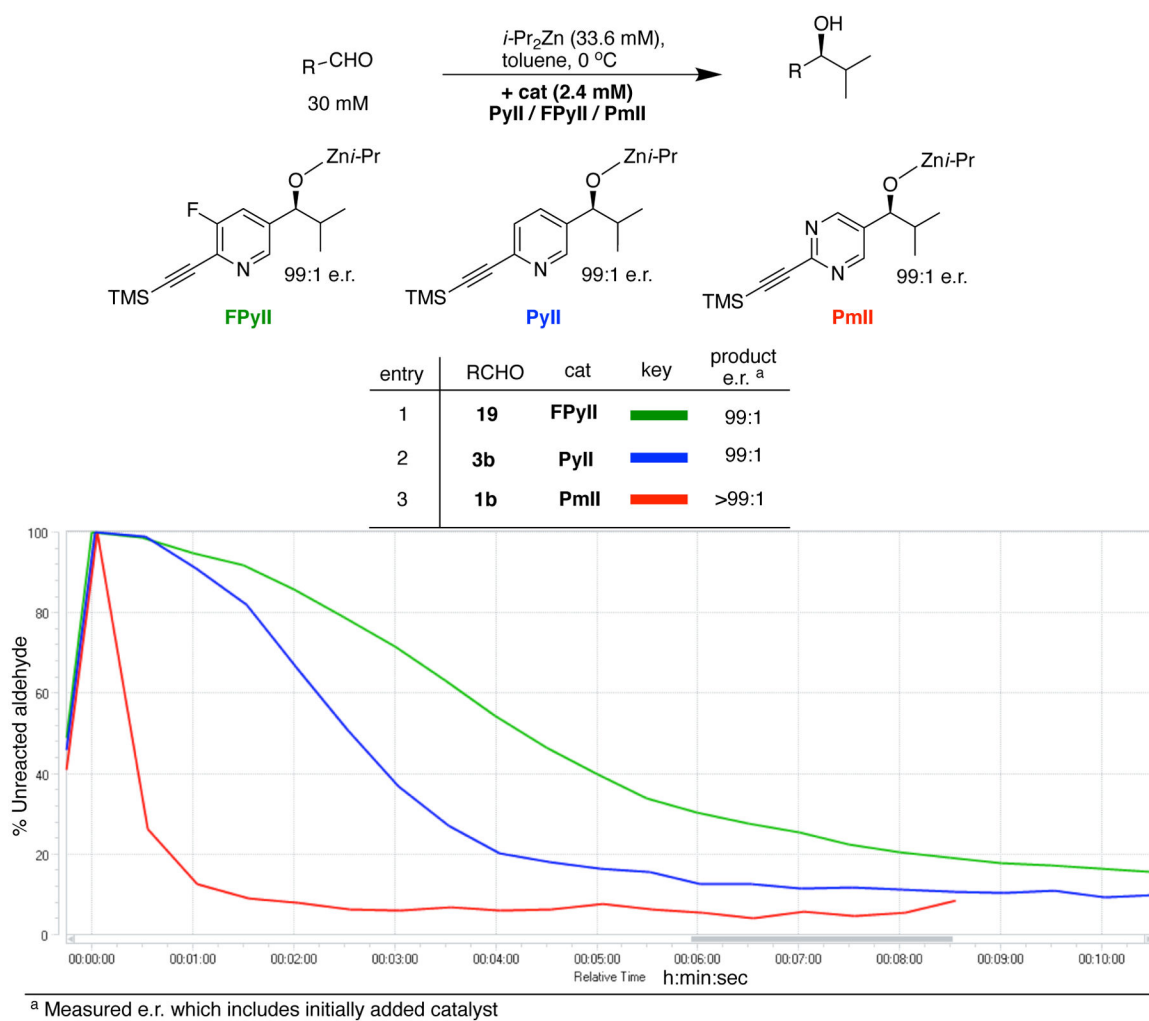
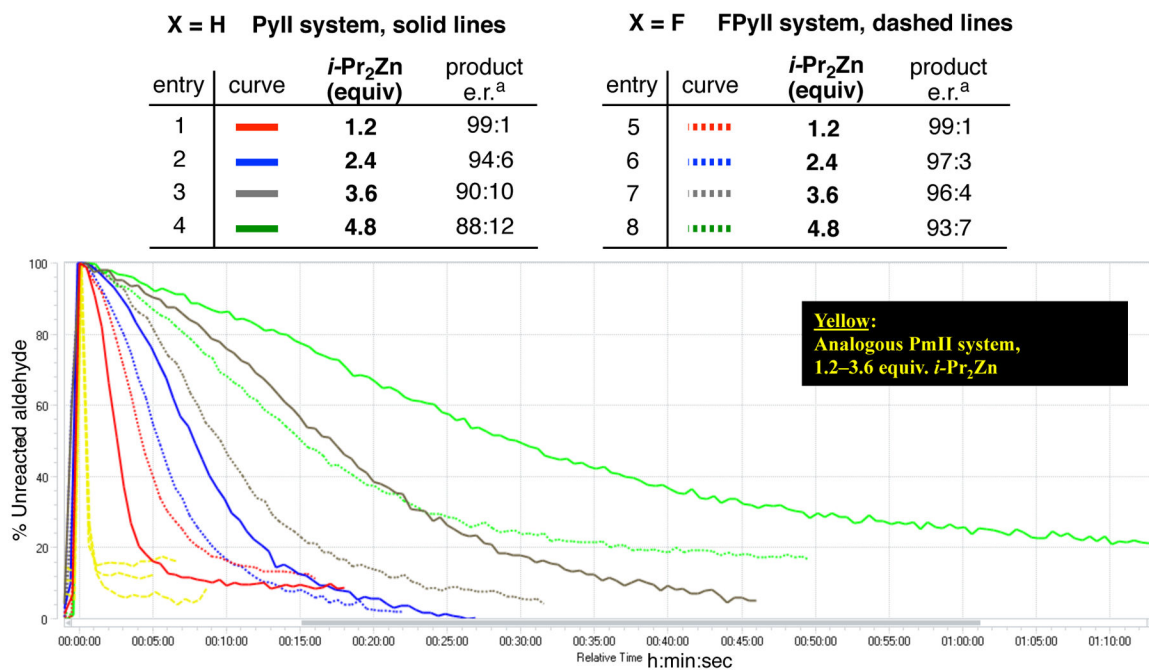
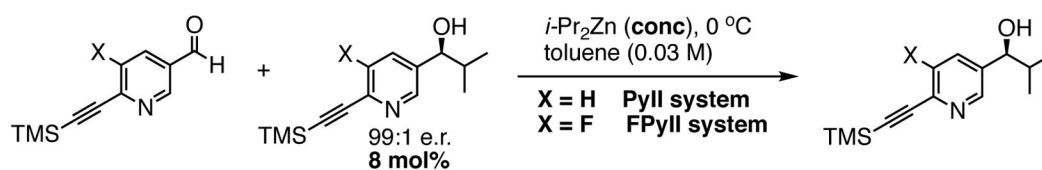


**Figure 14.**  
Comparison of autocatalytic progression in **PyII**, **FPyII** and **PmII** systems.



<sup>a</sup> Measured e.r. which includes initially added catalyst

**Figure 15.**  
 Inhibition of autocatalytic progression in **PyII**, and **FPyII** systems with increasing diisopropylzinc.

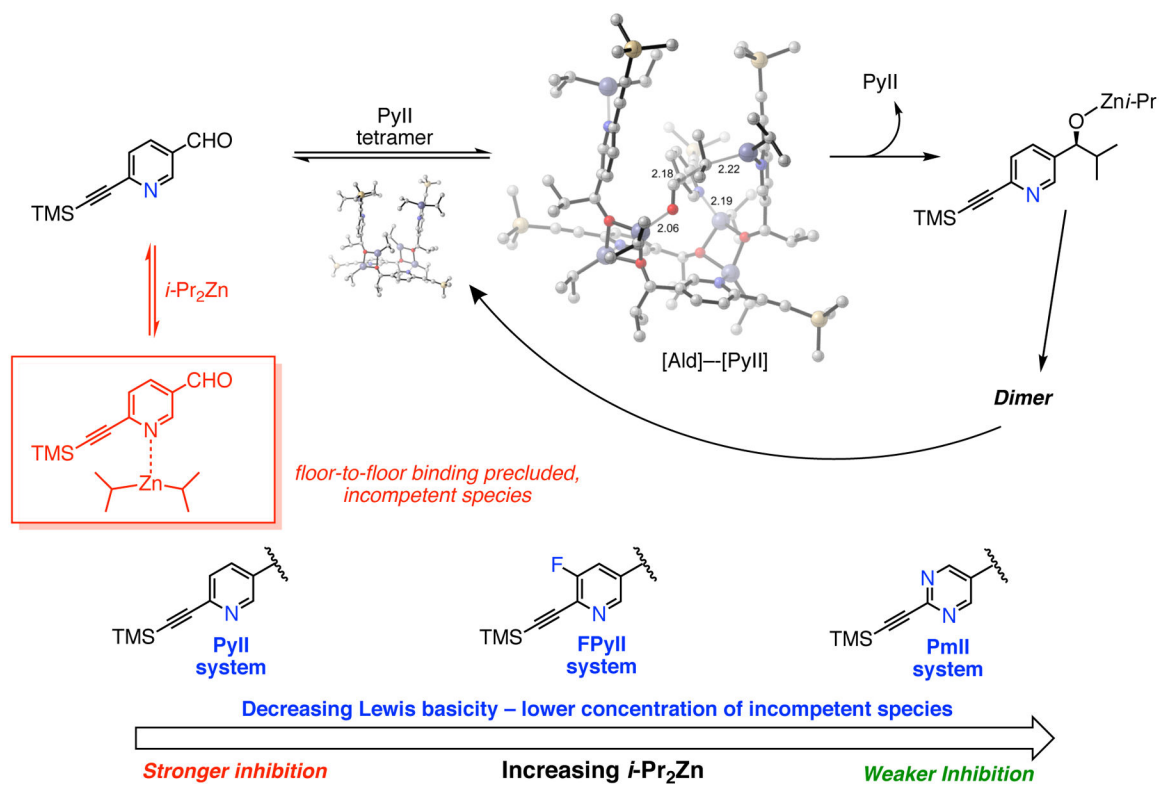
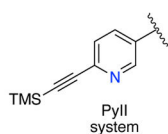
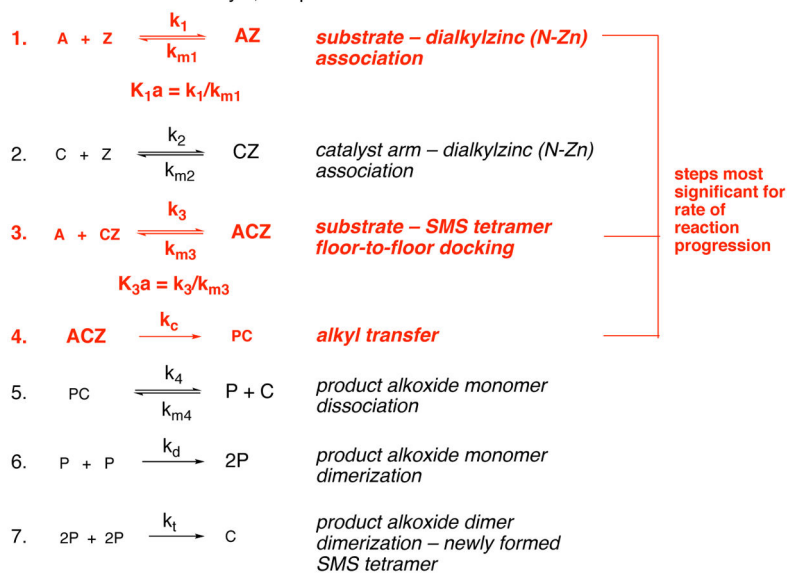


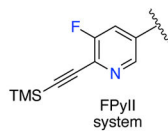
**Figure 16.** Schematic of the autocatalytic process (represented for the **PyII** system) and hypothesis for the origin of inhibition in the three systems.

**SF: a simplified reaction model for autocatalysis**

A = aldehyde, Z = Diisopropylzinc,  
 C = SMS tetrameric catalyst, P = product alkoxide monomer

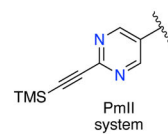


high value of  $K_1a$ ,  
maximal inhibition



intermediate value of  $K_1a$ ,  
reduced reagent inhibition

lower value of  $K_3a$  due to  
attenuated Lewis basicity?



low value of  $K_1a$   
faster reaction, minimal reagent  
inhibition

high value of  $k_c$  due to enhanced  
electrophilicity of the substrate?

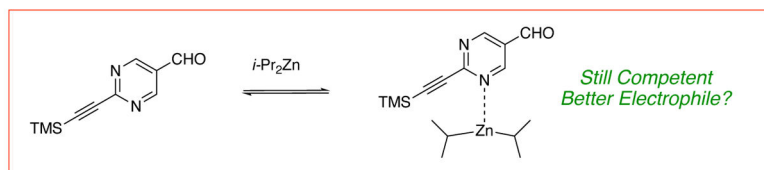
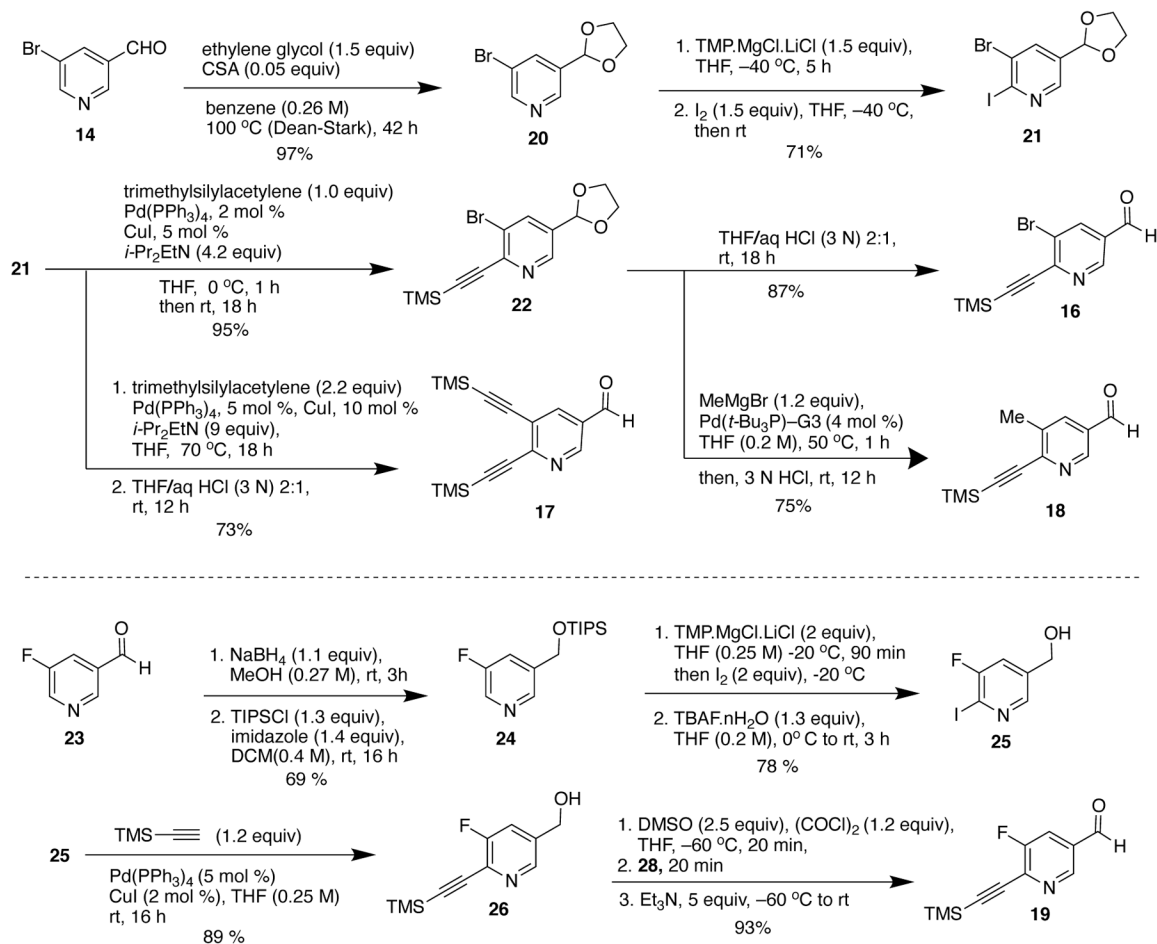


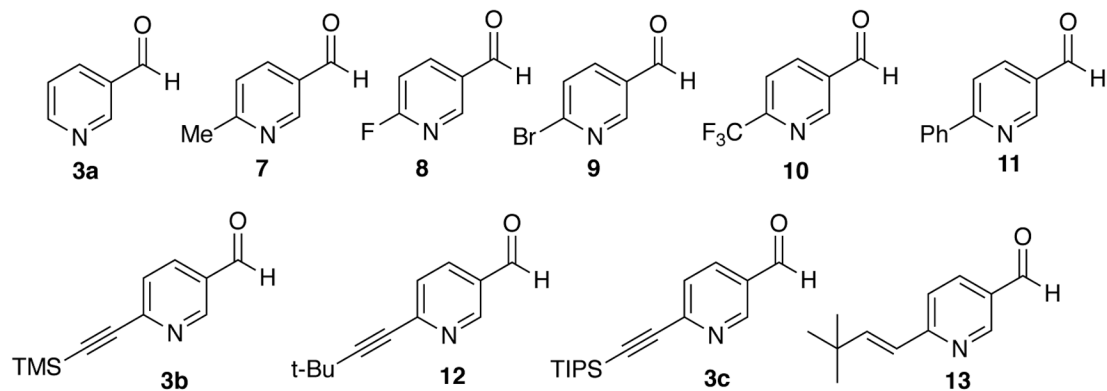
**Figure 17.**

The SF model of autocatalysis. Steps affecting rate of reaction progression are highlighted in red. The consequence of these steps in the **PyII**, **FPyII** and **PmII** systems are indicated.

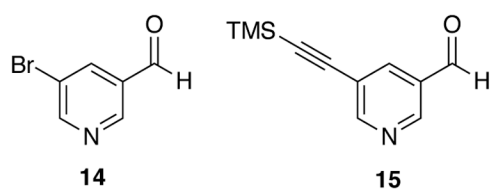


**Scheme 2.**  
 Synthesis of 5,6-disubstituted nicotinaldehydes.

## 6-substituted pyridine-3-carbaldehydes



## 5-substituted pyridine-3-carbaldehydes



## 5,6-disubstituted pyridine-3-carbaldehydes

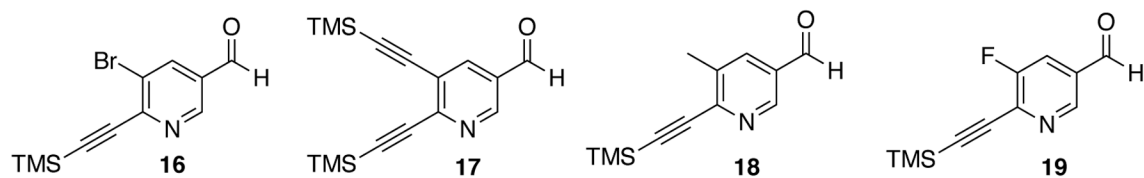


**Chart 1.**  
Substituted nicotinaldehydes tested for asymmetric autocatalysis with diisopropylzinc.